ORIGINAL ARTICLE

Plant, Cell & Environment PCE WILEY

Small paraquat resistance proteins modulate paraquat and ABA responses and confer drought tolerance to overexpressing Arabidopsis plants

Dóra Faragó[1] | Laura Zsigmond[1] | Dániel Benyó[1] | Rubén Alcazar[2] |
Gábor Rigó[1] | Ferhan Ayaydin[3,4] | Sahilu Ahmad Rabilu[1,5] |
Éva Hunyadi-Gulyás[6] | László Szabados[1]

[1]Institute of Plant Biology, Biological Research Centre, Szeged, Hungary

[2]Facultat de Farmàcia, Universitat de Barcelona, Barcelona, Spain

[3]Hungarian Centre of Excellence for Molecular Medicine (HCEMM) Nonprofit Ltd., Szeged, Hungary

[4]Cellular Imaging Laboratory, Biological Research Centre, Szeged, Hungary

[5]Doctoral School in Biology, Faculty of Science and Informatics, University of Szeged, Szeged, Hungary

[6]Proteomic Research Laboratory, Biological Research Centre, Szeged, Hungary

Correspondence
László Szabados, Institute of Plant Biology, Biological Research Centre, Temesvári krt. 62., 6726 Szeged, Hungary.
Email: szabados.laszlo@brc.hu

Abstract

Adaptation of higher plants to extreme environmental conditions is under complex regulation. Several small peptides have recently been described to modulate responses to stress conditions. The Small Paraquat resistance protein (SPQ) of *Lepidium crassifolium* has previously been identified due to its capacity to confer paraquat resistance to overexpressing transgenic Arabidopsis plants. Here, we show that overexpression of the closely related Arabidopsis SPQ can also enhance resistance to paraquat, while the Arabidopsis *spq1* mutant is slightly hypersensitive to this herbicide. Besides being implicated in paraquat response, overexpression of SPQs enhanced sensitivity to abscisic acid (ABA), and the knockout *spq1* mutant was less sensitive to ABA. Both Lepidium- and Arabidopsis-derived SPQs could improve drought tolerance by reducing water loss, stabilizing photosynthetic electron transport and enhancing plant viability and survival in a water-limited environment. Enhanced drought tolerance of *SPQ*-overexpressing plants could be confirmed by characterizing various parameters of growth, morphology and photosynthesis using an automatic plant phenotyping platform with RGB and chlorophyll fluorescence imaging. Our results suggest that SPQs can be regulatory small proteins connecting ROS and ABA regulation and through that influence responses to certain stresses.

KEYWORDS
abscisic acid, *Arabidopsis thaliana*, *Lepidium crassifolium*, plant phenotyping, stress tolerance

1 | INTRODUCTION

Proteins composed of less than 100 amino acids are classified as small proteins (SPs) and were largely ignored until recently due to the difficulties to identify, purify and characterize them with conventional molecular and biochemical tools. With the advance in genome sequencing and genome-wide transcriptome analysis, an increasing number of SPs have been discovered and characterized in several plants. In *Arabidopsis thaliana* (Arabidopsis) around 7000 small expressed genes have been identified, many of which can encode small regulatory proteins (Takahashi et al., 2019). Such signalling peptides can be recognized by membrane-bound receptor-like kinases (RLKs) initiating intracellular signalling events, and act similarly to phytohormones regulating plant development and plant–microbe or environmental interactions (Bartels & Boller, 2015; Fiume et al., 2016; Kereszt et al., 2018; Yamaguchi & Huffaker, 2011). Molecular and functional understanding of interactions of SPs with RLKs or other regulatory–regulatory proteins is however limited (Kim et al., 2021). SPs can influence responses to environmental stresses such as high salinity, dehydration, heat or oxidative stress generated by reactive oxygen species (ROS) (Bartels & Boller, 2015; Kim et al., 2021; Vie et al., 2017). The INFLORESCENCE DEFICIENT IN ABSCISSION (IDA) has 77 amino acids that mediate drought-induced leaf abscission (Patharkar & Walker, 2016). The Arabidopsis IDA-LIKE peptides IDL6 and IDL7 were shown to act as negative regulators of ROS signalling in biotic and abiotic stresses (Vie et al., 2017). They can downregulate several stress-induced genes including *ZAT10* and *ZAT12*, key regulators of ROS signalling. Other peptides with stress regulatory function are the CLAVATA3/ESR-RELATED (CLE) peptides, which are implicated in drought tolerance. CLE9 promotes stomatal closure in water-limiting conditions through stimulating H_2O_2 synthesis, modulation activities of the MAP kinases MPK3/6, the abscisic acid (ABA) signalling component OST1 kinase and guard cell anion channel SLAC1 (Zhang et al., 2019). The CLE25 peptide is mobile and mediates dehydration signals from roots to leaves, thereby activating the *NCED3* gene, which encodes the rate-limiting enzyme of ABA synthesis, promoting ABA accumulation in drought conditions (Takahashi et al., 2018). RAPID ALKALINIZATION FACTOR (RALF) peptides mediate Ca^{2+} signalling and are involved in diverse regulatory processes such as salt and immune responses, root growth, pollen tube growth and guard cell movement (Blackburn et al., 2020). The LRR-RLK receptor kinase FERONIA recognizes some RALF peptides and is necessary for salt-induced Ca^{2+} signal transduction and mediation between RALF peptides and ABA signals (Chen et al., 2016). Searching for genes that could be responsible for stress tolerance of the halophytic plant *Lepidium crassifolium*, we have isolated the *s*mall *p*araquat resistance protein (LSPQ), which enhanced resistance to paraquat in overexpressing Arabidopsis plants (Rigo et al., 2016). LcSPQ is composed of 69 amino acids and had an N-terminal signal peptide, suggesting that it can be targeted to the secretory pathway. LcSPQ has no sequence similarity to other known SPs, suggesting that it can be a novel type of regulator. These and other reports demonstrate that the complex but still unexplored world of plant SPs is important in defining stress tolerance traits.

Paraquat is a nonselective herbicide that exerts its toxic effect as an alternative electron acceptor of photosystem I, which blocks the reduction of ferredoxin and NADPH production, generating superoxide ions, hydrogen peroxide and other ROS. Production of ROS is the principal reason for paraquat toxicity causing redox imbalance and oxidative stress, leading to the peroxidation of lipids and other macromolecules (Hawkes, 2014; Lascano et al., 2012). Photosynthetic machinery is the main target of paraquat in green plants; however, this herbicide can also damage the mitochondrial electron transport system by producing superoxide and causing mitochondrial oxidative stress in nonphotosynthetic plant tissues and also in the yeast and mammalian cells (Cochemé & Murphy, 2008; Cui et al., 2019). Due to its ability to generate ROS, paraquat has been used to study the physiological consequences of oxidative stress (Lascano et al., 2012).

Resistance to paraquat has evolved in a number of weeds due to long-term exposure to this herbicide (Gressel, 1984; Yu et al., 2007). Magnitude and mechanism of paraquat resistance varied among species and collected accessions, suggesting that various cellular or physiological mechanisms can be responsible for resistance including compromised uptake, sequestration from the chloroplast and other organelles to vacuoles or enhancement of ROS detoxification and scavenging (Hawkes, 2014; Jóri et al., 2007; Preston et al., 1991; Shaaltier et al., 1988; Szigeti et al., 2001). Paraquat has a similarity to certain polyamines and can compete with the uptake of putrescine and cadaverine, but not spermidine (Hart et al., 1992). The Arabidopsis amino acid permease RMV1 functions as a polyamine carrier and its overexpression can confer hypersensitivity to both paraquat and polyamines by promoting the uptake of these compounds (Fujita et al., 2012). PDR11 is a plasma membrane-localized ABC transporter that transports paraquat but not polyamines. The *pdr11* mutant has reduced paraquat uptake and enhanced tolerance (Xi et al., 2012). PAR1 is a Golgi-localized L-amino acid transporter that enhances paraquat sensitivity upon overexpression (Dong et al., 2016; Li et al., 2013). Spermidine synthase-overexpressing Arabidopsis has higher polyamine content, enhanced stress tolerance and reduced paraquat sensitivity (Kasukabe et al., 2004). Paraquat sequestration can reduce exposure to sensitive target tissues such as meristematic regions or prevent uptake into the chloroplast (Lasat et al., 1997; Norman et al., 1993; Szigeti et al., 2001; Yu et al., 2010). Specific transporters were suggested to be responsible for the vacuolar compartmentalization of this drug (Jóri et al., 2007).

Resistance to paraquat is often accompanied by enhanced tolerance to other oxidative agents and ROS-generating environmental conditions (Chiang et al., 2006; Cummins et al., 1999; Shaaltier et al., 1988). High antioxidant capacity can reduce oxidative damage imposed not only by paraquat but also by abiotic stresses such as salinity, drought, cold or high light (Badawi et al., 2004; Lee et al., 2007; Murgia et al., 2004; Yoshimura et al., 2004). Plants that overexpress ascorbate peroxidase (APX), superoxide dismutase

(SOD) or dehydroascorbate reductase (DHAR) can have increased paraquat resistance (Badawi et al., 2004; Kwon et al., 2002; Lee et al., 2007; Murgia et al., 2004). Enhanced levels of glutathione peroxidase (GPX) could increase tolerance to paraquat and salinity (Yoshimura et al., 2004). Paraquat-generated oxidative damage was shown to be reduced by ABA through the modulation of H_2O_2 signals (Ding et al., 2009; Hu et al., 2005; Zhou et al., 2014).

In this report, we show that SPQ-like proteins are present in all plants including Arabidopsis, where it is encoded by a single gene. The function of Arabidopsis and Lepidium SPQs seems to be conserved as both LcSPQ and AtSPQ could confer paraquat resistance to overexpressing plants. Both SPQs enhanced ABA sensitivity and increased drought tolerance of Arabidopsis. SPQs can represent a previously unknown class of signalling SPs, which are implicated in stress response regulation.

2 | MATERIALS AND METHODS

2.1 | Plant material

All Arabidopsis (A. thaliana (L.) Heynh.) transgenic lines and mutants had a Columbia-0 (Col-0) background. The T-DNA insertion line (SALK-014243) was obtained from the SALK collection (Salk Institute). Homozygous spq1 mutant was identified by PCR genotyping of the segregating lines with SPQ-F and SPQ-R primers (Table S1) in combination with T-DNA-specific LB primer as described (Szabados & Koncz, 2003).

2.2 | Gene cloning

Full-length AtSPQ (AT3G52105.1) cDNA was amplified with AtSPQ-F-sal and AtSPQ-R-sma primers, annealing to 5′- and 3′-untranslated regions (UTRs) of the cDNA, using Phusion High Fidelity polymerase (Thermo Fisher Scientific). The PCR fragment was cloned into SmaI–SalI restriction sites of the pBSK(+) vector and the nucleotide sequence was verified. Error-free cDNA was subcloned into the pENTR-2B Gateway vector at EcoRV and SalI sites and subsequently transferred into the pTCO27235S binary plant transformation vector (Rigo et al., 2016), using the Gateway LR Clonase Enzyme (Life Technologies). To generate C-terminal gene fusions with GFP, SPQ cDNA was amplified with 3′-specific primers without STOP codon and cloned into the pDOND207 vector. Error-free cDNA was used to generate 35S::LcSPQ-sGFP and 35S::AtSPQ-sGFP gene fusions in pGWB5 expression vector using LR Clonase™ II (Thermo Fischer Scientific). To generate C-terminal gene fusion with HA tag, cDNA was amplified with LcSPQ-CHiA-F and LcSPQ-CHiA-R primers, cloned in the pPILY HA-epitope fusion vector (Ferrando et al., 2000), sequenced and subcloned into the binary vector pTCO27235S. Gene constructs were verified by sequencing and introduced into wild-type Arabidopsis via in planta transformation using the GV3101/pMP90 Agrobacterium strain (Koncz et al., 1994).

Arabidopsis transformation was performed with the floral dip method as described (Clough & Bent, 1998).

2.3 | Growth assays

For in vitro growth assays, Arabidopsis seeds were surface sterilized and germinated on half-strength MS (Murashige and Skoog) medium containing 0.5% sucrose, 0.8% agar, pH 5.7 as described (Szabados et al., 2002). Plants were grown in growth chambers under 120 µmol m^{-2} s^{-1} photon flux density at 12/12 h light/dark cycle, in 22°C/18°C temperature in light/dark conditions. To evaluate paraquat or ABA sensitivity in vitro, 5-day-old seedlings were transferred to fresh media supplemented by paraquat (0.1 and 0.3 µM) or ABA (1, 2.5, 5, 10 and 20 µM). Plant growth was recorded by periodic imaging and rosette sizes, chlorophyll and anthocyanin contents were determined by image analysis using the PlantSize software (Faragó et al., 2018). Root growth was analysed on vertical agar plates supplemented by paraquat (0.05, 0.1 and 0.3 µM) or polyamines (600 µM putrescine, 200 µM spermidine or 400 µM spermine). Root lengths were measured on digital images with the ImageJ/Fiji software. To measure hypocotyl elongation, seeds were germinated on culture media supplemented with paraquat (0.1 and 0.2 µM) in the dark. Six-day-old seedlings were photographed and hypocotyl lengths were measured with the ImageJ/Fiji. For germination assay, seeds were plated on an agar-solidified medium supplemented with ABA (0.3, 1 and 3 µM). Germination was scored by green cotyledon emergence at daily intervals. Each plate contained 50–100 seeds. Experiments were repeated three times.

2.4 | Measurement of stomatal apertures

Stomatal aperture was measured on leaves of 4–6-week-old soil-grown Arabidopsis plants. At least 10 leaves were harvested for each genotype and treatment and the peeled epidermis was incubated on the surface of sterile water containing 25 mM KCl, 10 mM MES-Tris, pH 6.15, and supplemented by ABA (1, 10 and 50 µM) for 3 h. The epidermis was subsequently photographed with a Nikon ECLIPSE TE300 microscope equipped with SPOT-RT II camera. The width and length of stomata (n = 50–55) were measured with ImageJ/Fiji. Experiments were repeated two times.

2.5 | Drought assays

Drought tolerance was tested in growth chambers at 22°C, 8/16 h light/dark cycle, ~150 µmol m^{-2} s^{-1} photon flux density or in the greenhouse under natural light conditions. Arabidopsis plants were cultured in plastic pots containing 110 g of soil for 3 weeks. Drought stress was applied by withholding water for 11–16 days. The relative water content (RWC) of drying plants was determined as described (Barr & Weatherley, 1962). Dehydrated plants were rewatered and

the number of green, surviving plants was counted 4–6 days after rewatering. To determine survival rates, 50–120 plants were used for each genotype and treatment, depending on the experiment. Experiments were repeated six times.

2.6 | Measurement of photosynthetic activity

Photosynthetic capacity was assessed by measuring electron transport rate (ETR), maximum photosystem II (PSII) quantum efficiency (F_v/F_m) and quantum yield of PSII (Φ_{PSII}) of drought-treated and control plants using Imaging-PAM (M-Series, Maxi version; Heinz Walz GmbH) (Baker, 2008). Plants were adapted to dark for 15 min before imaging. ETR was determined on the base of a rapid light curve, which was used for the calculation of fluorescence parameters at a photosynthetic photon flux density of 0, 56, 111, 186, 281, 336 and 396 μmol m^{-2} s^{-1} light intensities. Two leaf areas were selected on each plant and 20 plants were measured for each genotype. Experiments were repeated four times.

2.7 | Gene expression study

Total RNA was isolated from 100 mg Arabidopsis seedling or different plant organs using GeneJET Plant RNA Purification Mini Kit (Thermo Scientific, K0801). 5 of RNA was treated with TURBO DNA-free™ Kit (Thermo Fisher Scientific) and then 1 μg RNA was used for cDNA Synthesis using the High Capacity cDNA Reverse Transcription Kit (Applied Biosystems). Real-time PCR was carried out with the ABI 7900 Fast Real-Time System (Applied Biosystems) using SYBR Green qPCR Master Mixes (Thermo Scientific) following the manufacturer's instructions. Relative transcript levels were standardized to UBC18 (AT5G42990), ACT2 (AT3G18780) or 18S RNA as reference genes and calculated by the $2^{-\Delta Ct}$ or $2^{-\Delta\Delta Ct}$ method (Livak & Schmittgen, 2001). At least two biological replicates were made.

2.8 | Physiological measurements

2.8.1 | Determination of hydrogen peroxide content

H_2O_2 content was measured in 2-weeks-old plants using the Amplex Red Hydrogen Peroxide/Peroxidase Assay Kit (Thermo Fisher Scientific; A22188) as recommended by the manufacturer. Fifty milligrams of fresh plant material was harvested ($n = 5$ for all genotypes and treatments), ground in liquid nitrogen and resuspended in 20 mM potassium phosphate buffer (pH 6.5). The homogenates were centrifuged and the accumulation of resorufin in the supernatant was determined spectrophotometrically at 560 nm (Multiscan Go Microplate Spectrophotometer; Thermo Scientific). The amount of H_2O_2 was calculated using a standard curve. Experiments were repeated three times.

2.8.2 | Lipid peroxidation assay

Lipid peroxidation was measured by thiobarbituric acid-reactive substance assay. One hundred micrograms of leaf tissues were homogenized ($n = 5$ for all genotypes and treatments) with 1 ml of 0.1% trichloroacetic acid containing 0.4% butylhydroxytoluene. After centrifugation at 13 000 rpm for 20 min, 250 μl of supernatant was mixed with 1 ml 20% trichloroacetic acid containing 0.5% thiobarbituric acid and the mixture was incubated at 96°C for 30 min. Absorbance was read by Multiskan GO microplate reader (Thermo Fisher Scientific) at 532 nm and adjusted by nonspecific absorbance measured at 600 nm. Malondialdehyde concentration was calculated by using the extinction coefficient $\varepsilon 532 = 155$ mM^{-1} cm^{-1}. Five biological replicates were measured, and experiments were repeated two times.

2.8.3 | Proline content

Free proline concentrations were determined by the ninhydrin-based colorimetric assay as described (Abraham et al., 2010). The absorbance of the reaction product was determined spectrophotometrically at 520 nm using Thermo Scientific, Multiscan Go Microplate Spectrophotometer. Proline concentration was calculated with a standard curve. Five biological replicates were measured for each genotype and treatment. Experiments were repeated three times.

2.8.4 | Polyamine analysis

Polyamine concentrations were determined by high-performance liquid chromatography (HPLC) as described (Alcazar et al., 2005; Marcé et al., 1995).

2.9 | Cell fractionation and immunoblotting

Cellular extracts were prepared from transgenic Arabidopsis plants expressing the 35S::LcSPQ-HA, 35S::LcSPQ-GFP or 35S::AtSPQ-GFP constructs. Cellular fractions were separated by differential centrifugation as described (Baba et al., 2018). Twenty-five micrograms of total protein extract from each sample was size separated on 14% sodium dodecyl sulphate-polyacrylamide gel electrophoresis, transferred onto Immobilon PVDF Membrane (Millipore), incubated for 1 h in 1×TBST blocking buffer (50 mM Tris-HCl (pH 8.0), 150 mM NaCl, 0.05% Tween-20, 5% dry skimmed milk) and for 1.5 h with anti-GFP (11814460001; Roche) or anti-HA (11867423001; Roche) antibodies to detect the GFP- or HA-tagged SPQ proteins, respectively. ARF1 was detected with antibody Agrisera AS08325 and Agrisera AS10710 was used to detect histone H3. After washing with 1×TBST three times for 10 min, the membranes were incubated for 1.5 h with an anti-mouse-POD or anti-rabbit-POD secondary antibodies (dilution 1:5000; Pierce), washed with 1×TBST as before, and then

overlaid with Immobilon Western Chemiluminescent HRP Substrate (Millipore) for chemiluminescent detection by autoradiography or Fusion FX5 system (Vilber Lourmat).

2.10 | Confocal microscopy

In vivo localization of LcSPQ-GFP and AtSPQ-GFP was studied in 6–9-day-old seedlings. Plantlets expressing the 35S::LcSPQ-GFP and 35S::AtSPQ-GFP constructs were imaged using Visitron spinning disk confocal system having Yokogawa CSU-W1 spinning disk unit (pinhole diameter, 50 μm), Andor Zyla 4.2 Plus camera and Olympus IX83 inverted microscope (Visitron Systems GmBH). Laser excitation of 488 nm, fluorescence emission detection of 500–550 nm and ×60 oil (NA 1.42) and ×100 oil (NA 1.45) immersion objectives were used for imaging. Images were processed with Corel Photopaint (X7) software.

2.11 | Identification of SPQ-interacting proteins

SPQ-HA-overexpressing seedlings (0.5 g) were frozen in liquid nitrogen and extracted as described (Kobayashi et al., 2015). Total protein extracts (4 mg/immunoprecipitation) were precleaned using anti-GFP antibody and immunopurified using anti-HA antibody coupled with very small magnetic beads (MACS® Technology; Miltenyi) and digested in column with trypsin. The resulting tryptic peptide mixture was desalted on a C18 ZipTip (Omix C18 100 μl tips; Varian). The purified peptide mixture was analysed by liquid chromatography with tandem mass spectrometry (Hubner et al., 2010) using a nanoflow reversed-phase high-performance liquid chromatography (LC programme: linear gradient of 3%–40% B in 100 min; solvent A: 0.1% formic acid in water; solvent B: 0.1% formic acid in acetonitrile) on-line coupled to a linear ion trap-Orbitrap (Orbitrap-Fusion Lumos; Thermo Fisher Scientific) mass spectrometer operating in positive ion mode. Data acquisition was carried out in a data-dependent fashion, multiply charged ions were selected in cycle time from each MS survey scan for ion-trap higher-energy C-trap dissociation fragmentation (MS and MSMS spectra were acquired in the Orbitrap; R = 60 000). Raw data were converted into peak lists using the in-house Proteome Discoverer (v1.4) and searched against the Uniprot *A. thaliana* database (downloaded 2019.6.12, 89 461 proteins) using our in-cloud Protein Prospector search engine (v5.15.1) with the following parameters: enzyme: trypsin with maximum 1 missed cleavage; mass accuracies: 5 ppm for precursor ions and 10 ppm for fragment ions (both monoisotopic); fixed modification: carbamidomethylation of Cys residues; variable modifications: acetylation of protein N-termini; Met oxidation; cyclization of N-terminal Gln residues, allowing maximum two-variable modifications per peptide. Acceptance criteria: minimum scores: 22 and 15; maximum E values: 0.01 and 0.05 for protein and peptide identifications, respectively. Spectral counting was used to estimate the relative abundance of individual proteins in the indifferent antibody (GFP) negative controls and in the anti-HA immunopurified samples (Jankovics et al., 2018).

2.12 | Plant phenotyping

Wild-type Col-0 and LcSPQa, LcSPQb, AtSPQa and AtSPQb lines were analysed with the PlantScreen™ Compact System (Photon System Instrument [PSI]) phenotyping system, following an established protocol (Awlia et al., 2016). Plants were cultured in individual pots filled with equal amounts of sewed Plantobalt Substrate 1 soil (https://www.plantaflor.de/en/products/propagation/details/plantobalt-substrate-1-fine-80-20-clay). Culture conditions were the following: 8 h/16 h, 22°C/20°C in light/dark cycle and relative humidity of 65%. Light-emitting diode illumination was employed: cool white (5700 K) completed with deep red (660 nm, 30%), blue (470 nm, 20%), Far Red (740 nm, 30%), ultraviolet (UV) (405 nm, 20%) with 130 μmol m^{-2} s^{-1} photon irradiance. Plants were grown for 21 days after sowing then watering of drought-stressed plants was stopped for 22 days, followed by rewatering to allow recovery (Figure S12). Plants were subjected to automatic phenotyping during dehydration and recovery periods at daily intervals. One round of measurement included chlorophyll fluorescence (ChlF) and RGB imaging, followed by weighing and watering. RGB imaging was made with a top view 12.36 Megapixels GigE PSI RGB camera with 1.1" CMOS sensor (Sony IMX253LQR-c, 4112 × 3006 resolution). ChlF images were captured with FluorCam FC-800MF Pulse Amplitude-modulated (PAM) system (pixel resolution of 1360 × 1024, frame rate 20 fps and 16-bit depth). Fluorescence imaging was made after 15 min of dark adaptation, followed by the protocol: 5 s of pulse-modulated short duration measuring flashes with red-orange 620 nm light at 33 μs (Fo), 800 ms of saturation pulse with cool-white light at 1200 μmol m^{-2} s^{-1} irradiance in the dark-adapted state (F_m), 180 s intervals of cool-white actinic light at 130 μmol m^{-2} s^{-1}. Thirty plants were analysed for each genotype and treatment. PSI PlantScreen™ Data Analyser software (PSI) was used for image processing and retrieving of raw data, which were subsequently processed by RStudio software. The dynamic responses between genotypes were characterized and identified outliers (1.5× interquartile range) were removed from the curated data set. Statistical analysis was made with MVApp application performing analysis of variance (ANOVA) (Kruskal–Wallis) with pairwise Wilcoxon's test/Mann–Whitney's test of significance with $p < 0.05$ (Julkowska et al., 2019).

2.13 | Bioinformatics and computing

Protein sequences were retrieved from Phytozome (https://phytozome.jgi.doe.gov). Multiple sequence alignment was made with Clustal Omega (https://www.ebi.ac.uk/Tools/msa/clustalo/). Sequence domains were identified with SMART (http://smart.embl-heidelberg.de). Phylogenetic tree, gene constructs and primers were

designed with CLC Main Genomics Workbench (https://www.qiagenbioinformatics.com/products/clc-genomics-workbench/). Root or hypocotyl sizes were measured with ImageJ/Fiji (https://imagej.net/Fiji). Rosette sizes and anthocyanin contents were determined by PlantSize (http://www.brc.hu/pub/psize/index.html) (Faragó et al., 2018). Transcript data were compiled from the Genevestigator database (https://genevestigator.com/gv/). Phenotyping data were processed by RStudio (https://www.r-project.org) and MVApp (https://github.com/mmjulkowska/MVApp).

Statistical analyses (t test, one- and two-way analysis of variance ANOVA, means comparisons by Tukey's tests) were performed using the OriginPro 2018 software version 9.5 (OriginLab Corporation, Northampton, MA, USA). In case of one-way ANOVA the differences between means were determined by Duncan's multiple range test and labelled in a diagram with different letters. Data were processed with MS Excel 14.7.7.

3 | RESULTS

3.1 | Identification of *SPQ* gene and protein in Arabidopsis

LcSPQ conferred paraquat resistance in overexpressing Arabidopsis plants (Rigo et al., 2016). Sequence homology search revealed that similar genes are present in one or two copies in the genome of all higher plants which encode proteins of 66–76 amino acids (Figures 1, S1 and S2). In Arabidopsis, the *AT3G52105* gene is most closely related to LcSPQ, with two annotated spliced RNA variants encoding proteins of 70 or 110 amino acids. The *AT3G52105.1*-encoded protein has the highest degree of sequence similarity to the LcSPQ protein (92% identity) and was named AtSPQ. An N-terminal signal peptide but no other well-defined domain could be identified in the SPQ-type proteins (Figure 1a). The *AT3G52105.1* transcript is present in all plant organs and each developmental stage of Arabidopsis (Figures 1b and S3). Transcript analysis of *AtSPQ* and *LcSPQ* genes in Arabidopsis and in *L. crassifolium*, respectively, showed only minor alterations in oxidative, osmotic and salt-stressed plants, suggesting that SPQ genes are not stress-regulated (Figure S4).

3.2 | Intracellular localization and interactions of SPQ

To study the intracellular localization of Arabidopsis- and Lepidium-derived SPQ proteins, HA- and GFP-tagged LcSPQ and AtSPQ were expressed in transgenic Arabidopsis plants under the control of the CaMV35S promoter. Western detection of SPQ-HA and SPQ-GFP fusions in fractionated cell extracts revealed that SPQ protein is most abundant in the microsomal fraction that includes Golgi, endomembranes, endoplasmic reticulum and plasma membrane (Figure S5). Confocal microscopy showed that SPQ-GFP-derived fluorescence

(a)

(b)
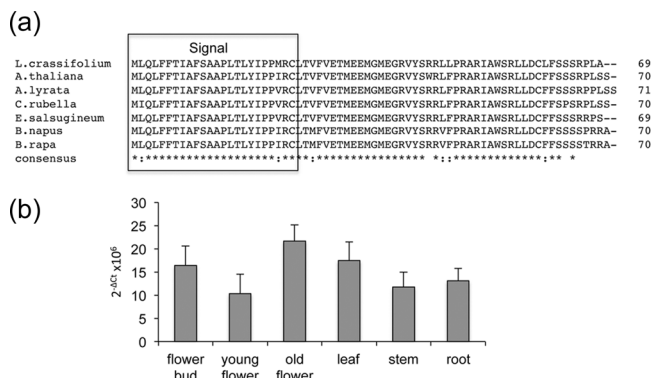
FIGURE 1 Analysis of SPQ-type proteins. (a) Multiple sequence alignment of seven SPQ proteins of species from the Brassicaceae family. (b) Expression of *AtSPQ* in Arabidopsis. Quantitative RT-PCR was used to determine transcript levels in various organs of Col-0 wild-type plants. Relative expression is shown as $2^{-\Delta Ct} \times 10^6$, comparing *AtSPQ* transcript levels to 18S RNA used as reference. RT-PCR, reverse transcription-polymerase chain reaction; SPQ, small paraquat resistance protein.

was associated with tonoplast, cytoplasmic vesicles and membranous intracellular structures, but was absent in nuclei, intravacuolar space, on the plasma membrane or cell wall (Figures S6 and S7). Results obtained with AtSPQ-GFP and LcSPQ-GFP fusions gave identical results. Microscopic observations could confirm data obtained with cell fractionation and suggest that SPQ proteins are located in close proximity to membraneous structures.

To study the molecular function of SPQ, proteins, which can interact with HA-tagged LcSPQ were identified in an immunoprecipitation experiment coupled with mass spectrometry. Twelve Arabidopsis proteins could be identified in two biological replicates with at least two unique peptide count values (Table S1). The identified proteins are implicated in various cellular and biological processes such as modulation of the cytoskeleton, membrane transport and endomembrane trafficking, regulation of vesicle formation, redox control, hormone and defence regulation. An RLK-like kinase was among the identified SPQ interactors, suggesting that this receptor may be implicated in SPQ recognition. These results suggest that SPQ can modulate cellular processes through interaction with other proteins.

3.3 | Overexpression of Arabidopsis SPQ enhances paraquat tolerance

To compare the functions of LcSPQ and AtSPQ proteins, full-length cDNA of *AT3G52105* was cloned and overexpressed in Arabidopsis under the control of the CaMV35S promoter. Plants overexpressing LcSPQ have already been described (Rigo et al., 2016). In vitro growth assays revealed that overexpression of LcSPQ and AtSPQ could confer paraquat resistance to Arabidopsis plants (Figures 2a and S8). Paraquat-induced oxidative damage was prevented by LcSPQ and AtSPQ overexpression as lipid peroxidation
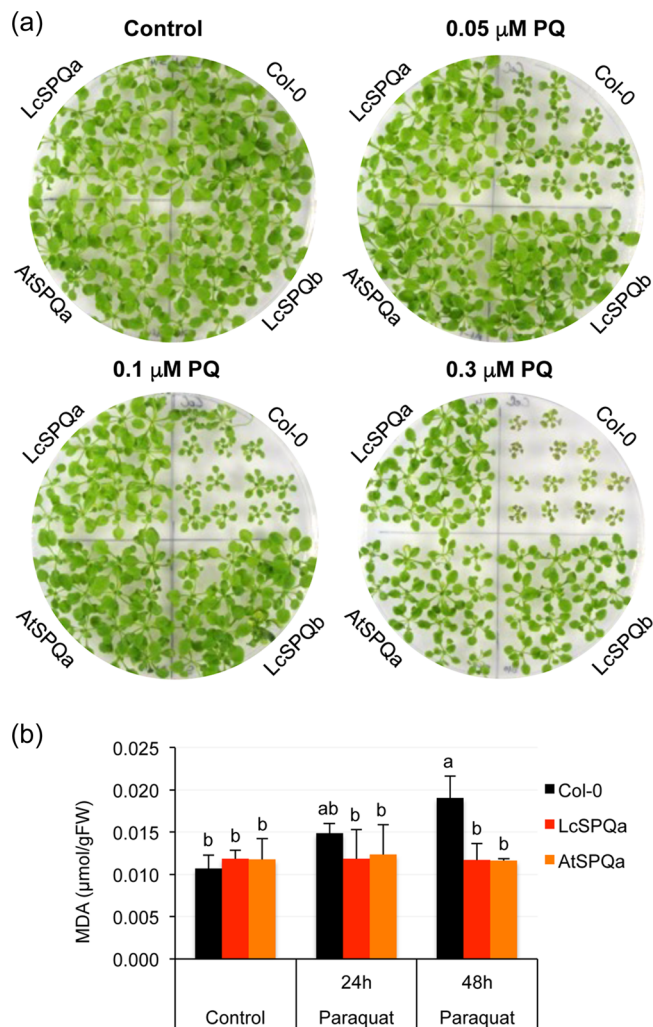
FIGURE 2 Paraquat resistance of SPQ-overexpressing plants. (a) Growth of Col-0 and homozygous LcSPQ- and AtSPQ-overexpressing on paraquat-containing culture media. Images of 3-week-old plants are shown. (b) Lipid peroxidation rates of Col-0- and SPQ-overexpressing plants. Two-week-old plantlets were treated with 7 µM paraquat and incubated for 24 or 48 h before measuring MDA content. Bars on diagrams indicate standard deviation. Statistically significant differences are indicated by different letters, $p < 0.05$ (one-way ANOVA, means comparison by Tukey's test). ANOVA, analysis of variance; SPQ, small paraquat resistance protein.

did not increase in paraquat-treated transgenic plants (Figure 2b). We concluded that AtSPQ and LcSPQ overexpression can similarly confer paraquat tolerance to Arabidopsis.

To characterize the function of the *AT3G52105* gene in more detail, a T-DNA insertion mutant has been characterized. In the SALK_014243 mutant, an inverted repeat of T-DNA is inserted in the *AT3G52105* exon, six nucleotides downstream of the ATG (*spq1*). Compared to Col-0 wild type, the *AT3G52105* transcript was greatly reduced in the homozygous *spq1* mutant (Figure 3a). The growth of the *spq1* mutant was comparable to Col-0. Minor phenotypic alterations were observed, which included elongated petioles

(Figure 3b). TAIR gene models suggest that a 150 nucleotide 3′ overlap exists between the transcripts of *AT3G52105.1* and the neighbouring reverse complementary *AT3G52110* genes, which encodes an unknown protein (Figure S9A). To test whether the expression of these genes is modulated by the 3′ overlap, their transcript levels were determined in the overexpressing AtSPQa plants and in the *spq1* mutant. Reverse transcription-polymerase chain reaction (RT-PCR) revealed that *AT3G52105* transcript was absent in the mutant, is enhanced in the overexpressing AtSPQa plants, while expression of *AT3G52110* was comparable in these genotypes (Figure S9B). These data excluded the possibility that transcript interference such as small interfering RNA-mediated silencing of *AT3G52110* is responsible for the phenotype of SPQ-overexpressing plants. To test the paraquat sensitivity of the *spq1* mutant, seedlings were grown in various concentrations of this herbicide (Rigo et al., 2016). Growth inhibition of *spq1* by paraquat was similar to wild type when rosette sizes were compared, but higher anthocyanin accumulation in the *spq1* mutant indicated slight hypersensitivity to this drug (Figure 3b–d).

Paraquat is known to generate ROS and inhibit photosynthesis. To compare photosynthetic parameters of wild type, SPQ-overexpressing and *spq1* mutant plants, ChlF was tested in in vitro-grown plants. In control conditions, F_v/F_m and Φ_{PSII} were similar to wild-type plants. Paraquat reduced both F_v/F_m and Φ_{PSII} values of Col-0 and *spq1* mutant plants, but these parameters were not affected in the LcSPQa and AtSPQa plants (Figure S10). Paraquat and ROS are known to induce the expression of various genes and the *RCD1* gene is known to regulate such signals (Ahlfors et al., 2004). Induction of the ROS-induced *ZAT12* was inferior in SPQ-overexpressing plants and in the *spq1* mutant than in Col-0 plants, but *RCD1* expression was not different in these genotypes (Figure S11A). Reduced peroxide accumulation in SPQ-overexpressing plants (Figure 8a) can be responsible for the inferior activation of *ZAT12* in these plants.

Paraquat can block electron transport not only in chloroplasts but also in mitochondria and can therefore affect nonphotosynthetic organs. To compare paraquat sensitivity of wild type and LcSPQa, AtSPQa, *spq1* roots, their elongation was tested on paraquat containing media. Inhibition of root growth was reduced in SPQ-overexpressing plants, but was not significantly different in *spq1* when compared to wild type (Figure 4a,c). To test paraquat sensitivity in the absence of light, hypocotyl elongation of dark-germinated seedlings was compared. Hypocotyl elongation of etiolated Col-0 and *spq1* seedlings was similarly reduced by paraquat, but was less affected in AtSPQa and LcSPQa plants (Figure 4b,d). Growth reduction of *spq1* was comparable to wild type in both illuminated and dark-grown plants, while anthocyanine accumulation was higher in mutant leaves in light (Figures 3 and 4). These results indicate that overexpression of both Arabidopsis and Lepidium SPQ can confer resistance to paraquat not only in light but also independently of photosynthesis, and the mutation has only a minor effect on paraquat toxicity in growth assays.
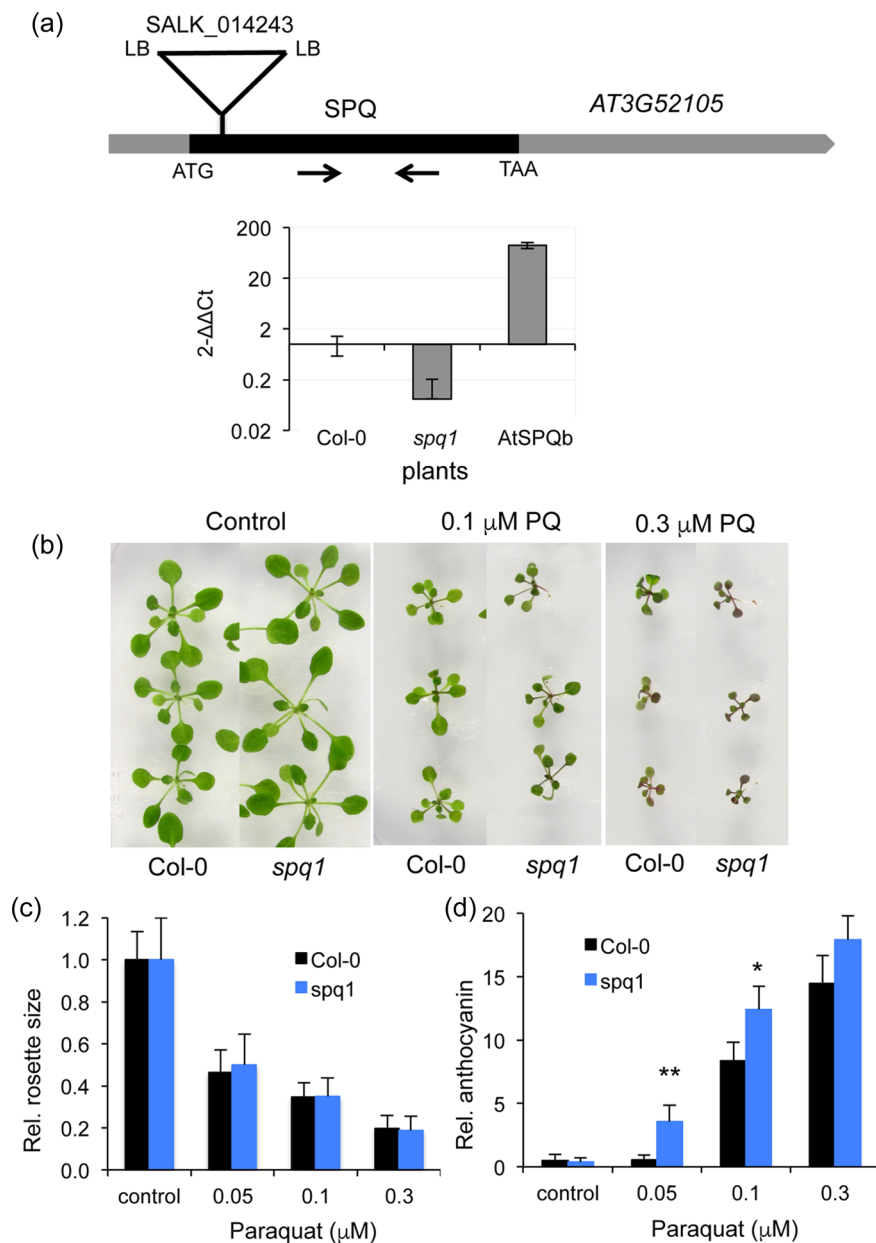
FIGURE 3 Paraquat response of the *spq1* mutant. (a) Schematic map of the *AT3G52105* gene with the T-DNA insertion in SALK_014243. The position of the PCR primers used for qRT-PCR reactions is shown. qRT-PCR analysis of the *SPQ* gene in Col-0, *spq1* mutant and AtSPQb line. (b) Col-0 and *spq1* plants are grown on paraquat-containing media. Five-day-old seedlings were transferred to a culture medium containing paraquat and grown for 10 days. Rosette size and anthocyanin content were determined on colour images using PlantSize (Faragó et al., 2018). (c) Relative growth of Col-0 and *spq1* rosettes. The growth rate was normalized to plants grown on control media. (d) Relative anthocyanin content of Col-0 and *spq1* plants. 1 corresponds to values detected on control plates. Bars on diagrams indicate standard deviation, * and ** show significant differences of *spq1* to Col-0 at $p < 0.05$ and $p < 0.01$, respectively (Student's *t* test). qRT-PCR, quantitative reverse transcription-polymerase chain reaction; SPQ, small paraquat resistance protein. [Color figure can be viewed at wileyonlinelibrary.com]

3.4 | Polyamine metabolism is not altered in SPQ-overexpressing plants

Paraquat uptake can be mediated by the polyamine transport system and polyamine metabolism was implicated in some form of paraquat resistance (Fujita et al., 2012; Kurepa et al., 1998). To test whether polyamine metabolism is modulated by SPQ, the polyamine content of LcSPQa, AtSPQa and *spq1* plants was tested. Polyamines were found to modulate stress responses through crosstalk with ABA signalling and ABA was shown to influence polyamine metabolism (Dong et al., 2016; Marco et al., 2011). As ABA sensitivity of SPQ-overexpressing and mutant plants was altered (see below), ABA treatment was included in these assays. Spermine content was higher in the presence of paraquat, and putrescine was accumulating more in ABA-treated plants. Differences in polyamine contents of

SPQ-overexpressing and mutant plants, however, could not be revealed, suggesting that SPQ does not interfere with polyamine metabolism (Figure S12A). High concentrations of polyamines were shown to inhibit root growth (Dong et al., 2016; Fujita et al., 2012). To evaluate the effect of SPQ on polyamine sensitivity, root growth of SPQ overexpressing and mutant plants were tested in the presence of putrescine, spermidine and spermine. Even though root growth was reduced by these polyamines, genotype-specific differences were not observed (Figure S12B). Polyamine uptake is mediated by several membrane transporters which can transport paraquat also. The expression of main polyamine transporter genes PUT2 (AT1G31830), PUT3 (AT5G05630) and PDR11 (AT1G66950) was therefore tested in SPQ overexpressing and *spq1* mutant plants. Although paraquat slightly enhanced the expression of these genes, transcript levels were similar in the tested genotypes (Figure S11B).

FIGURE 4 Paraquat sensitivity of nonphotosynthetic organs. (a) Root growth of Col-0, LcSPQa and AtSPQa lines and the *spq1* mutant in the presence of paraquat. (b) Hypocotyl elongation of etiolated LcSPQa and AtSPQa and *spq1* seedlings. Seeds were germinated on paraquat containing culture media in the dark. Hypocotyl lengths were measured 5 days after germination. (c) Average root lengths. (d) Average hypocotyl lengths of seedlings. Scale bar = 1 cm. Bars on diagrams indicate standard deviation; * show significant differences to Col-0 at *p* < 0.05 (*n* = 30, two-way ANOVA, means comparison by Tukey's test). ANOVA, analysis of variance. [Color figure can be viewed at wileyonlinelibrary.com]
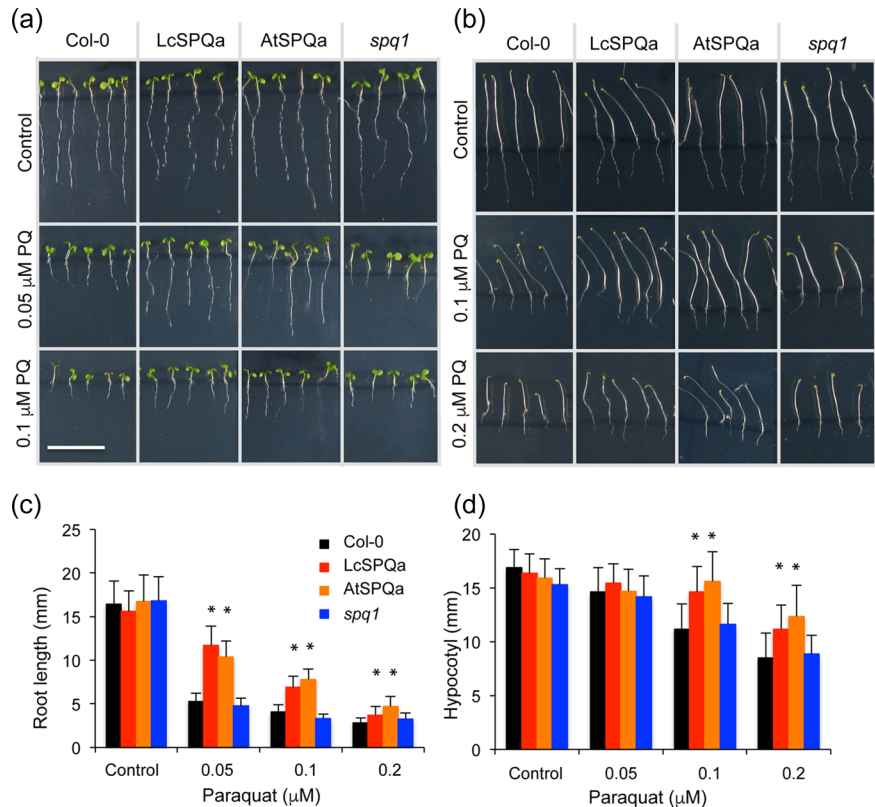
These results suggest that SPQ does not interfere with polyamine transport and SPQ-dependent paraquat resistance is independent of polyamine metabolism.

3.5 | ABA response is modulated by SPQ

Paraquat generates ROS, which can interfere with stress response regulation and ABA signalling (Ding et al., 2009; Zhou et al., 2014). To examine the influence of SPQ on ABA regulation, ABA sensitivities of SPQ-overexpressing and *spq1* mutant plants were tested. Growth was compared on culture media supplemented with various concentrations of ABA. Rosette sizes of the tested lines were similar to the standard culture medium. SPQ-overexpressing plants were however smaller, and the *spq1* mutant was larger than the wild type in the presence of ABA (Figure 5a,b). Chlorophyll content was reduced by 30%–40% in SPQ-overexpressing plants in the presence of 1 or 2.5 μM ABA and was higher by 30%–100% in the *spq1* mutant on media containing 2.5, 5 or 10 μM ABA than in wild-type plants (Figure 5a,c). Sensitivity to ABA was further tested in germination assays, scoring germination frequencies on ABA-containing media. *spq1* germination was slightly insensitive to ABA, but LcSPQa and AtSPQa seeds germinated similarly to wild type (Figure S13).

To test whether SPQ is implicated in ABA-controlled transcriptional regulation, expression of the *RD29A* (*AT5G52310*) and *RAB18* (*AT5G66400*) genes was monitored in SPQ-overexpressing plants and the *spq1* mutant. These genes are known to be induced by drought and ABA signals and can be used to monitor stress responses at the molecular level (Lång & Palva, 1992; Msanne et al., 2011). *RD29A* and *RAB18* were clearly induced by 6 h of ABA treatment, which was further enhanced by SPQ overexpression. After 24 h of ABA treatment, transcript levels of *RAB18*, but not *RD29A*, were still higher in SPQ-overexpressing plants, but were not altered in the *spq1* mutant (Figure 6a).

Leaf epidermal guard cells have key importance in the control of evaporation during water restriction regulated by ABA through promoting stomata closure. Mutations that modulate the ABA sensitivity of guard cells have a profound effect on respiration, water loss and drought tolerance (Finkelstein, 2013; Mustilli et al., 2002). Therefore, the influence of SPQ on stomatal closure was tested. Stomatal aperture was similar in all plants in control conditions and was significantly smaller in ABA-treated guard cells of SPQ-overexpressing plants. Stomata aperture of the *spq1* mutant remained larger than wild type only when a high ABA concentration was used (Figure 6b,c). These results revealed that LcSPQ and AtSPQ overexpression enhances ABA sensitivity, while the *spq1* mutant is slightly insensitive to ABA.

3.6 | SPQ overexpression enhances drought tolerance

Enhanced ABA sensitivity of the SPQ-overexpressing plants prompted us to investigate responses to water limitation and drought. As ABA and paraquat sensitivities of the *spq1* mutant were not particularly different from wild-type plants, the mutant was not
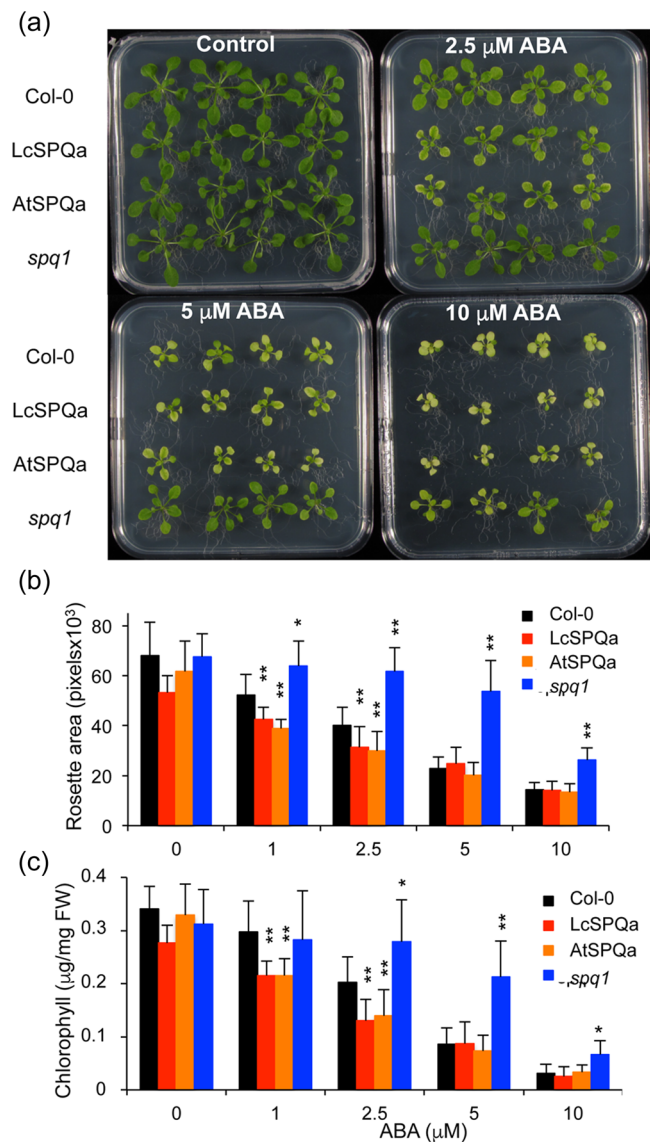
FIGURE 5 Growth of LcSPQ- or AtSPQ-overexpressing and *spq1* mutant plants on ABA-containing culture media. Seeds were germinated on a standard culture medium and 7-day-old seedlings were transferred to the culture medium supplemented by ABA. (a) Images of plants grown on ABA-containing and control media for 10 days. Rosette sizes (b) and chlorophyll content (c) of plants grown on ABA-containing media. Rosette area and chlorophyll contents were determined by analysing colour images with PlantSize (Faragó et al., 2018). Bars on diagrams indicate standard deviation, * and ** show significant differences to Col-0 at $p < 0.05$ and $p < 0.01$, respectively (Student's *t* test). ABA, abscisic acid. [Color figure can be viewed at wileyonlinelibrary.com]

included in these experiments. Tolerance to drought was characterized by eliminating watering of soil-grown plants cultured either in the greenhouse or in growth chambers and scoring recovery rate after rewatering. The results of a typical greenhouse experiment are shown in Figure 7. Change in soil water content was estimated by periodic measurement of pot weights (Figure 7b). Drought-exposed plants were rewatered after 16 or 21 days of water withdrawal, when

relative pot weights dropped to 25% or 20%, implying mild or severe stress, respectively. RWC of leaves was less reduced in SPQ-overexpressing plants (Figure 7b). Plant survival rate was scored 7 days after rewatering by calculating the ratio of recovered, green plants with visible turgor and healthy leaves (Figure 7c). Mild and severe drought stress reduced survival rates of Col-0 plants to 30%–10%, respectively. SPQ overexpression leads to significantly superior survival in both mild and severe stress conditions. Fifty percent to 80% of SPQ-overexpressing plants survived mild stress, and 25%–70% could recover after severe drought (Figure 7d). Experiments were repeated three times in the greenhouse and three times in growth chambers. Although survival rates were different in individual experiments, they were always superior in SPQ-overexpressing plants than in wild type (Figure S14).

To better understand the physiological and molecular background of the drought tolerance of SPQ overexpressing plants, several stress-related parameters were studied in drought-treated plants. When plants were exposed to water stress, the RWC of wild-type and SPQ-overexpressing plants was similar to wild-type plants until the ninth day of drying and then it was reduced to 25% in Col-0 and to 50%–55% in SPQ-overexpressing plants, respectively (Figure 8a). Proline accumulation is a well-characterized response to osmotic stress and other adverse conditions (Szabados & Savoure, 2010). Proline content was 5 and 30 times enhanced in wild-type plants on the 9th and 11th day of drought, respectively. Proline accumulation in SPQ-overexpressing plants was 40%–50% lower than in wild-type plants in such conditions (Figure 8b). Accumulation of ROS in many abiotic stresses is a consequence of damaged electron transport and insufficient scavenging capacity. H_2O_2 content increased in Col-0 plants 1.5 and 3.5 times after exposure to drought for 9 and 11 days, respectively, and it was only slightly enhanced in SPQ-overexpressing plants (Figure 8c). ROS can exert oxidative damage to macromolecules and lipid membranes, which was assessed by measuring MDA contents. We observed a slight increase in MDA content in the wild-type plants upon exposure to drought stress for 9 days and the level was increased five times after 11 days. When compared to wild type, lipid peroxidation was reduced by 50%–60% in SPQ-overexpressing plants, which correlated with their inferior H_2O_2 accumulation (Figure 8c,d). Photosynthesis is one of the most drought-sensitive metabolic processes, which can be monitored by measuring ETR using chlorophyll fluorescence detection (Sperdouli & Moustakas, 2011). Accurate determination of ETR involves Φ_{PSII} at a given PAR, a portion of incident PAR absorbed by PSII and the equal absorbance of PAR by leaf. Therefore, it is an appropriate stress indicator, especially in drought conditions (Baker, 2008). In well-watered conditions, ETR was not significantly different between wild-type and SPQ-overexpressing plants. ETR was considerably reduced in all drought-treated plants, but remained significantly higher in SPQ-overexpressing plants than in Col-0 (Figure 8e). These data suggested that both LcSPQ and AtSPQ overexpression can alleviate oxidative damage of drought-stressed plants by containing ROS accumulation and stabilization of the photosynthetic electron transport system in water-limited conditions.

FIGURE 6 ABA sensitivity of wild-type, LcSPQ- or AtSPQ-overexpressing plants and the *spq1* mutant. (a) Expression of ABA-induced genes RAB18 and RD29A in ABA-treated and control plants. Two-week-old in vitro-grown plants were treated with 50 μM ABA and transcript levels were determined by qRT-PCR using actin2 and UBC10 reference genes. Relative expression is shown where 1 corresponds to transcript levels of Col-0 in 6 h control samples. Averages of three biological repetitions are shown. Bars on diagrams indicate standard deviation, * shows significant differences to Col-0 at $p < 0.05$ (Student's *t* test). (b) Stomata opening of SPQ-overexpressing and mutant lines. Typical images of control and ABA-treated guard cells from leaf epidermis of Col-0, LcSPQa, AtSPQa and *spq1* plants. Scale bar = 20 μm. (c) Ratio of stomata diameter and length indicates the degree of stomata opening. Larger numbers indicate more open stomata. Bars on diagrams indicate standard deviation, * show significant differences to Col-0 at $p < 0.05$ (one-way ANOVA, means comparison by Tukey's test). ABA, abscisic acid; ANOVA, analysis of variance; SPQ, small paraquat resistance protein. [Color figure can be viewed at wileyonlinelibrary.com]
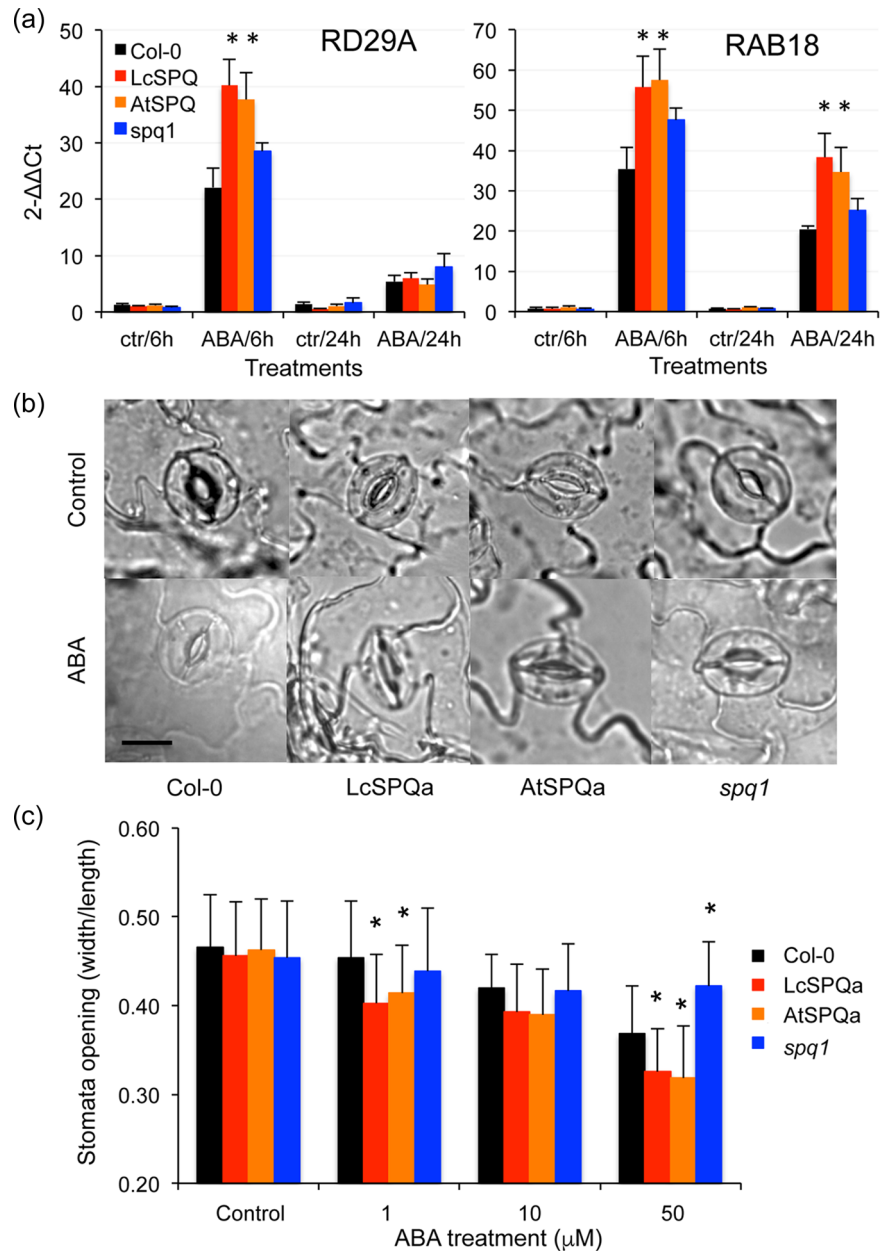
3.7 | Plant phenotyping confirms drought tolerance of SPQ-overexpressing plants

The application of image-based phenotyping facilitates simultaneous, nondestructive study of plant growth, morphology and photosynthesis, which are key traits to characterize plant stress tolerance (Awlia et al., 2016; Rungrat et al., 2016). Imaging allows repetitive detection in contrast to endpoint measurements of physiological traits. To monitor kinetic changes in plant growth and physiology in water-limiting conditions, wild-type and SPQ-overexpressing plants were analysed in controlled environmental conditions using a phenotyping platform (PSI). Plants were grown for 21 days after sowing, and watering was withdrawn for 22 days, followed by rewatering (Figure S15A). Soil water content diminished gradually until Day 22, when pots were rewatered (Figure S15B). Growth,

morphology and various physiological parameters of Col-0 wild-type and two AtSPQ- and two LcSPQ-overexpressing plants were monitored by RGB and ChlF imaging. Rosette areas were measured by determining green areas of colour-segmented RGB images of individual plants. Rosettes of well-watered Col-0 plants grew steadily in the imaging period. Water stress reduced the growth of green leaf areas, which declined 18 days after watering stopped. Rewatering on Day 22 of the drought allowed partial plant recovery (Figure S15C). As most dramatic changes happened between the 18th and 22nd day of water stress, comparative analysis of the different genotypes was focused on these days. The change of rosette areas of the wild-type and transgenic lines was similar in well-watered and water-limited conditions (Figures 9a and S16). Morphological differences could be observed in advanced drought conditions when the rosette roundness of wild-type plants declined faster than SPQs, indicating
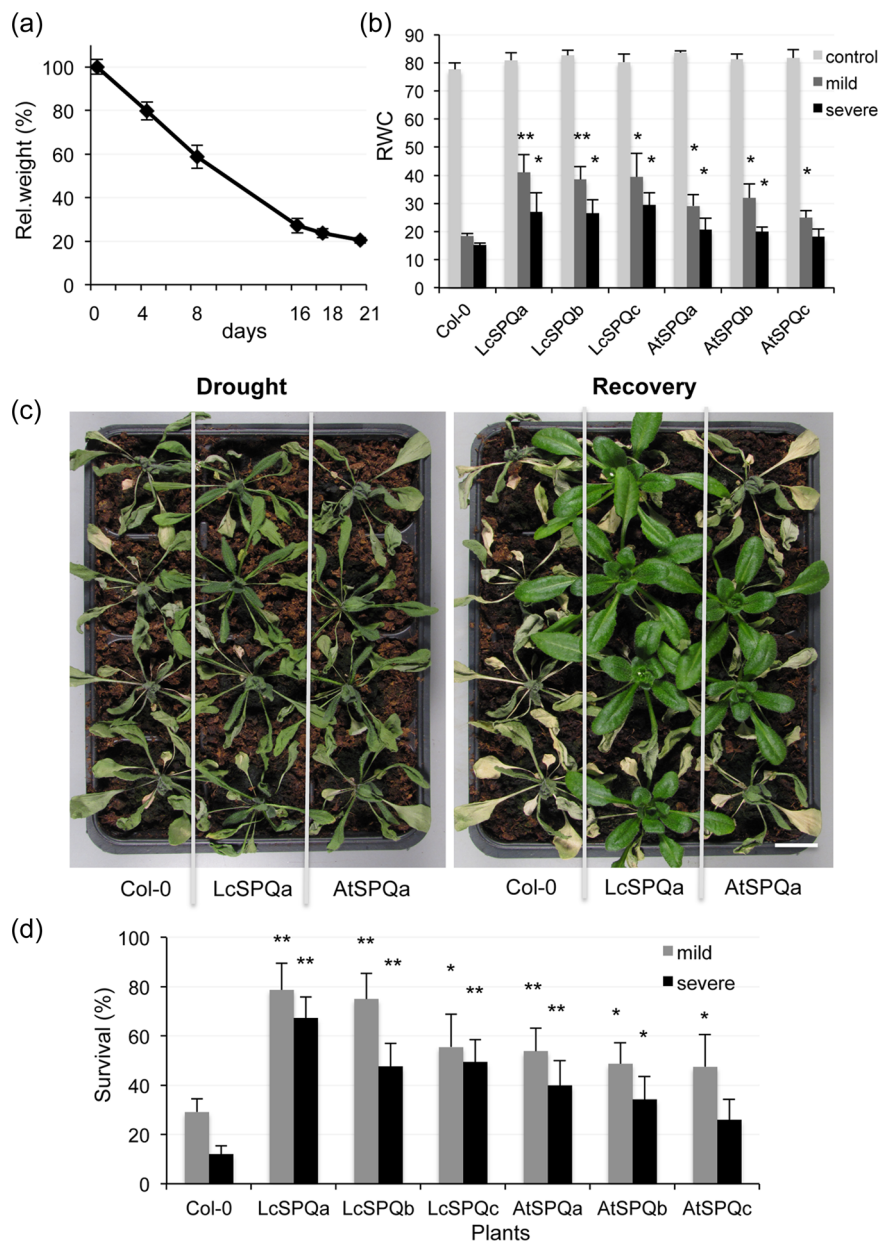
FIGURE 7 Drought tolerance of SPQ-overexpressing Arabidopsis plants. Plants were grown in a greenhouse and plants were subjected to drought stress by water withdrawal followed by rewatering. (a) Change of relative weight of pots after water withdrawal. (b) Relative water content (RWC) of drought-treated Arabidopsis plants. (c) Images of representative Col-0, LcSPQa and AtSPQa Arabidopsis plants exposed to drought and 7 days after rewatering. Scale bar =1 cm. (d) Survival rates of Arabidopsis plants subjected to mild (16 days) or severe (21 days) drought. The survival of 120 plants was scored for each genotype and treatment. Bars on diagrams indicate standard deviation, * and ** show significant differences to Col-0 at $p < 0.05$ and $p < 0.01$, respectively (Student's t test).

differences in loss of the regular rosette shape (Figure 9b). Rosette roundness describes a circular parameter comparing the rosette area to a perfect circle (Pavicic et al., 2017). RGB images were colour segmented into nine green hues to determine their abundance in rosette areas. Hue ratios were similar in well-watered plants, but considerable changes in hue abundances were observed in water-stressed plants. The proportioned share of hues 4 and 6 increased in drought-treated plants after 16 days of stress, which was reversed after rewatering. Changes in hue abundance were similar in all genotypes, although more marked differences were observed in AtSPQa and LcSPQa lines (Figure S17).

To compare the photosynthetic performance of well-watered and drought-stressed plants, ChlF imaging was performed at daily intervals in the detection period. F_v/F_m is considered a good indicator of photosynthetic capacity and its rapid decline during late phases of

dehydration was shown to reflect the loss of viability (Sperdouli & Moustakas, 2011; Woo et al., 2008). F_v/F_m values were similar (0.81–0.83) in all genotypes in well-watered conditions, and until 18–19 days after water withdrawal. Reduction of F_v/F_m values was, however, slower and happened 1–2 days later in SPQ-overexpressing plants than in Col-0, suggesting that transgenic plants retained their viability better (Figures 10a and S18). ETR declined also later in SPQ-overexpressing plants than in wild-type ones (Figure S19). When photochemical processes cannot utilize all absorbed photons, the excess excitation energy is dissipated through nonphotochemical quenching (NPQ), which can increase during severe drought conditions (Sperdouli & Moustakas, 2011; Woo et al., 2008). NPQ was similar in standard growth conditions in the genotypes tested and increased suddenly in wild-type plants after 20 days of water withdrawal, followed by a decline on Day 22. In SPQ-overexpressing

FIGURE 8 Physiological parameters of Col-0 wild-type and LcSPQ- or AtSPQ-overexpressing plants subjected to drought stress in the growth chamber. Relative water content (a), proline content (b), hydrogen peroxide levels (c) and lipid peroxidation were measured as MDA content (d) in leave samples of control and drought-stressed plants. Bars on diagrams indicate standard deviation, * show significant differences to Col-0 at $p < 0.05$ (one-way ANOVA, means comparison by Tukey's test, $n = 5$). (e) ETR of drought-treated and control plants exposed to drought for 12 days. Electron transport was measured by PAM imaging of 20 plants ($p < 0.05$, two-way ANOVA, means comparison by Tukey's test). ANOVA, analysis of variance. [Color figure can be viewed at wileyonlinelibrary.com]
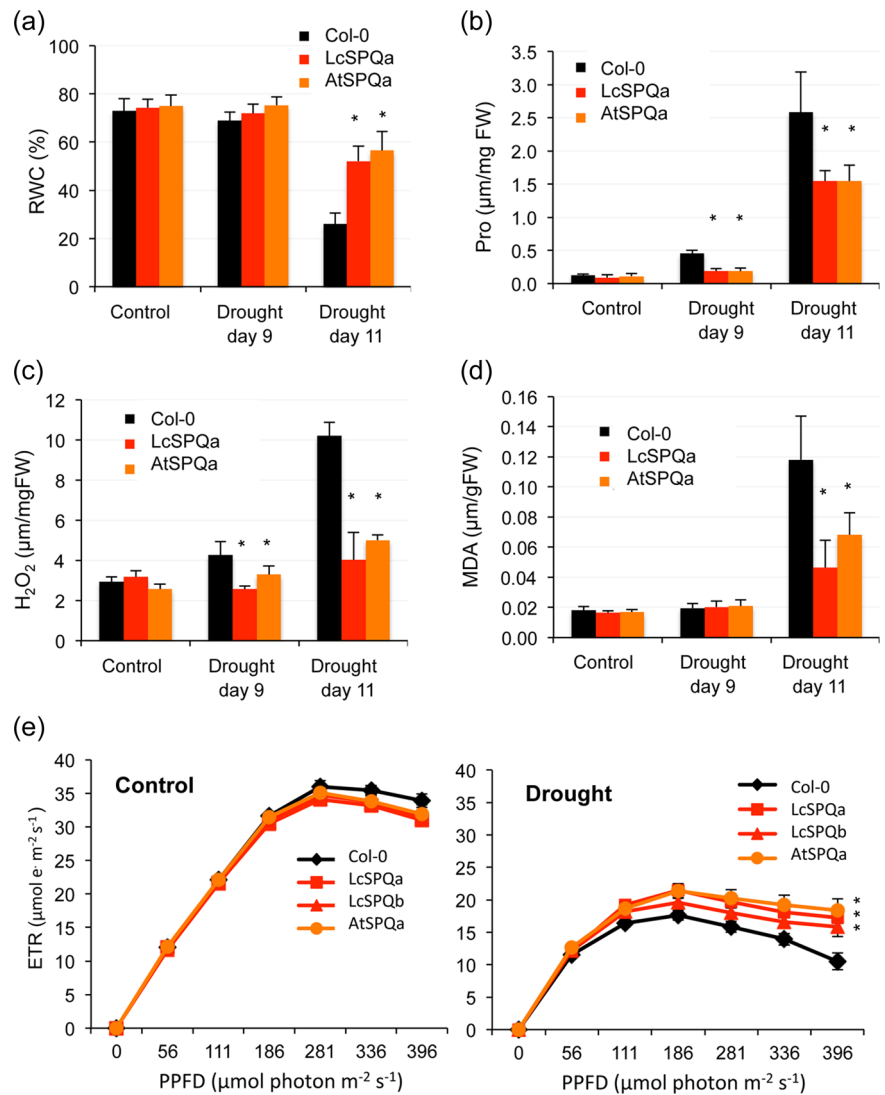
plants, NPQ increased only in more severe conditions on Day 22 (Figures 10b and S20). Phenotyping data revealed that in water-restricted conditions, morphological changes originated from wilting, and the decline of photosynthetic parameters was delayed in SPQ-overexpressing plants in comparison to wild-type Arabidopsis, indicating that SPQ can contribute to preserving viability in drought conditions.

4 | DISCUSSION

4.1 | Arabidopsis and Lepidium SPQ enhances resistance to paraquat

We have previously identified SPQ in the halophytic plant *L. crassifolium*, which increased paraquat resistance of overexpressing Arabidopsis plants (Rigo et al., 2016). SPQ-like genes exist in all plants in one or two copies, but none of them has been characterized. All SPQ-type proteins had a conserved signal sequence, but no other known protein domain. In Arabidopsis, the *AT3G52105* gene is the closest relative of the Lepidium SPQ, which was predicted to produce two splice variants *AT3G52105.1* and *AT3G52105.2*, encoding proteins of 8.1 and 13.7 kDa, respectively (Figures 1, S1, and S2). As *AT3G52105.1* was most related to LcSPQ (95% similarity), we have analysed the encoded protein of this splice variant and called it AtSPQ. The gene product of *AT3G52105* was predicted as a DIS3-exonuclease-like protein in the TAIR database. DIS3/SCAR2 is a large protein, composed of 1399 amino acids, implicated in trichome development. Such annotation, however, might be an error as no significant sequence similarity could be identified between the SPQ and DIS3 proteins by pairwise alignments (not shown). SPQ has no similarity with any of the SPs, which were implicated in the regulation of abiotic stress responses, suggesting that SPQs belong to a new class of regulators (Bartels & Boller, 2015; Kim et al., 2021; Vie et al., 2017).

Transcripts of the *AT3G52105* gene could be detected in low abundance in all tissues tested (Figures 1 and S3). Expression of the Arabidopsis and Lepidium SPQ genes was not influenced by salt,
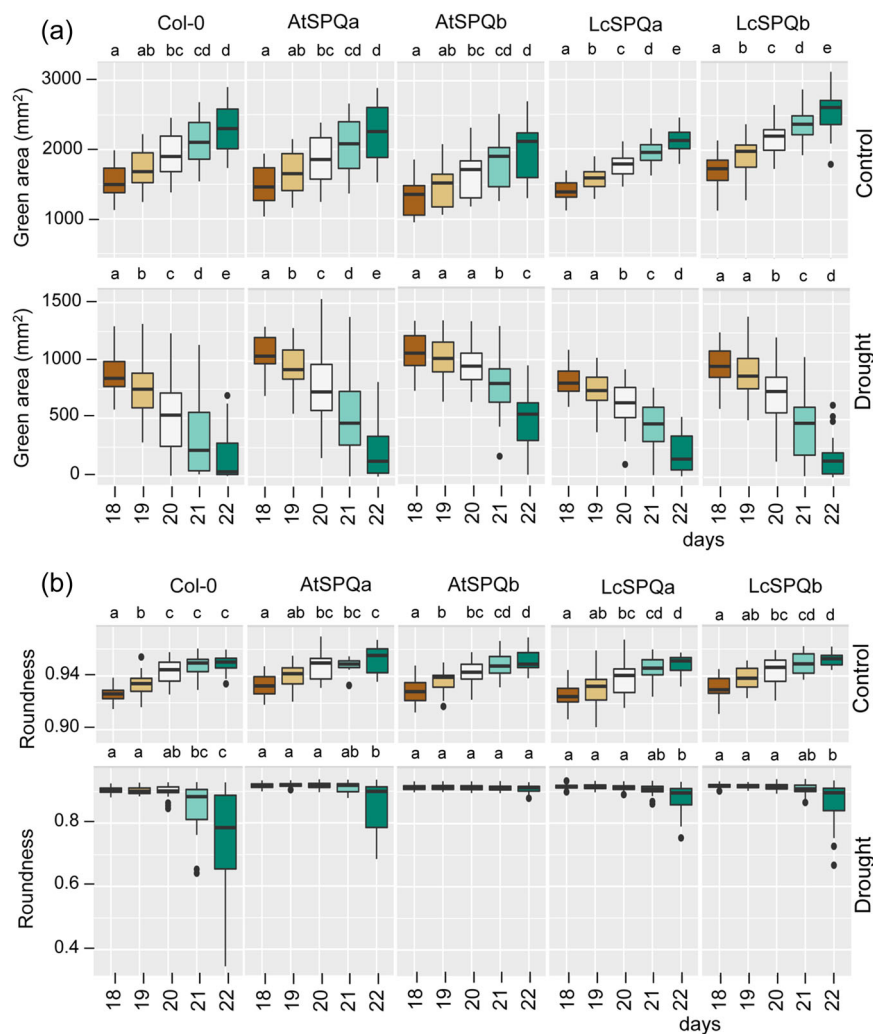
FIGURE 9 Growth of drought-stressed Arabidopsis plants, determined by plant phenotyping. Wild-type (Col-0) and SPQ-overexpressing plants (LcSPQa, b and AtSPQa, b) were grown in well-watered controlled growth conditions for 21 days, then watering was suspended for 22 days to generate gradual drought stress (control: uninterrupted watering; drought: water withdrawal, see Figure S12). RGB images of 30 plants were used to show average rosette sizes as green areas (a) and shape as roundness (b). Different letters indicate significant differences between the treatments and genotypes with analysis of variance (Kruskal–Wallis) with pairwise Wilcoxon's test/Mann–Whitney test of significance with $p < 0.05$. SPQ, small paraquat resistance protein. [Color figure can be viewed at wileyonlinelibrary.com]

osmotic or oxidative stresses (Figure S4), suggesting that these genes are not regulated by abiotic stress. SPQ could be detected in the microsomal fraction in cell fractionation experiments, suggesting that it is associated with membraneous cellular structures. Such observation could be confirmed by confocal microscopy, which detected SPQ-GFP in the tonoplast and endomembrane system (Figures S5–7). These data correspond to SUBA prediction, which suggests AtSPQ localization in endoplasmatic reticulum, Golgi or extracellular space. The N-terminal signal peptide SPQs (Figure 1) may direct such localization.

Overexpression of AtSPQ and LcSPQ in transgenic Arabidopsis greatly enhanced paraquat resistance (Rigo et al., 2016) (Figures 2 and S8). The fact that overexpression of both Lepidium- and Arabidopsis-derived SPQs was able to improve paraquat resistance suggests that their abundance and not a particular LcSPQ sequence defines such feature. In higher plants, the principal target of paraquat is photosynthesis, where this drug functions as an electron acceptor blocking ferredoxin reduction and disrupting electron transport. Toxicity is a consequence of the resulting ROS production, leading to oxidative damage (Hawkes, 2014; Lascano et al., 2012). SPQ overexpression could reduce paraquat-triggered damage

of photosynthesis and retain loss of PSII functions as confirmed by Φ_{PSII} or F_v/F_m values, which otherwise declined faster in paraquat-treated wild type plants (Figure S10). Notably, SPQ overexpression promoted resistance to paraquat not only in illuminated green plants but also in the dark-germinated, etiolated seedlings and roots (Figure 4), indicating that the protective effect of this protein is not confined to photosynthetic cells. Paraquat is toxic for nonphotosynthetic organisms such as animals or yeast, where it functions as an electron acceptor in mitochondria, disrupting mitochondrial electron transport-generating ROS (Blanco-Ayala et al., 2014; Cochemé & Murphy, 2008; Krall et al., 1988). In plants, paraquat can produce ROS also in nonphotosynthetic tissues or in the absence of light where mitochondria are the main target of toxicity (Bowler et al., 1991; Cui et al., 2019). Our results are in line with these results and demonstrate that SPQ alleviates paraquat-generated damage in both light and dark and in photosynthetic and nonphotosynthetic tissues.

Resistance to paraquat can originate from impaired uptake, enhanced sequestration or catabolism as well as from increased detoxification of ROS, generated in the damaged photosynthetic or mitochondrial electron transports (Hawkes, 2014). Sequence analysis of SPQ proteins, however, could not reveal any similarity to

FIGURE 10 Effect of drought stress on photosynthetic parameters of Col-0 wild-type and SPQ-overexpressing plants, determined by phenotyping and ChlF imaging. (a) F_v/F_m of control and drought-stressed plants. (b) NPQ of control and drought-stressed plants. Different letters indicate significant differences between the treatments and genotypes with analysis of variance (Kruskal–Wallis) with pairwise Wilcoxon's test/Mann–Whitney test of significance with $p < 0.05$. ChIP, chlorophyll fluorescence; NPQ, nonphotochemical quenching. [Color figure can be viewed at wileyonlinelibrary.com]
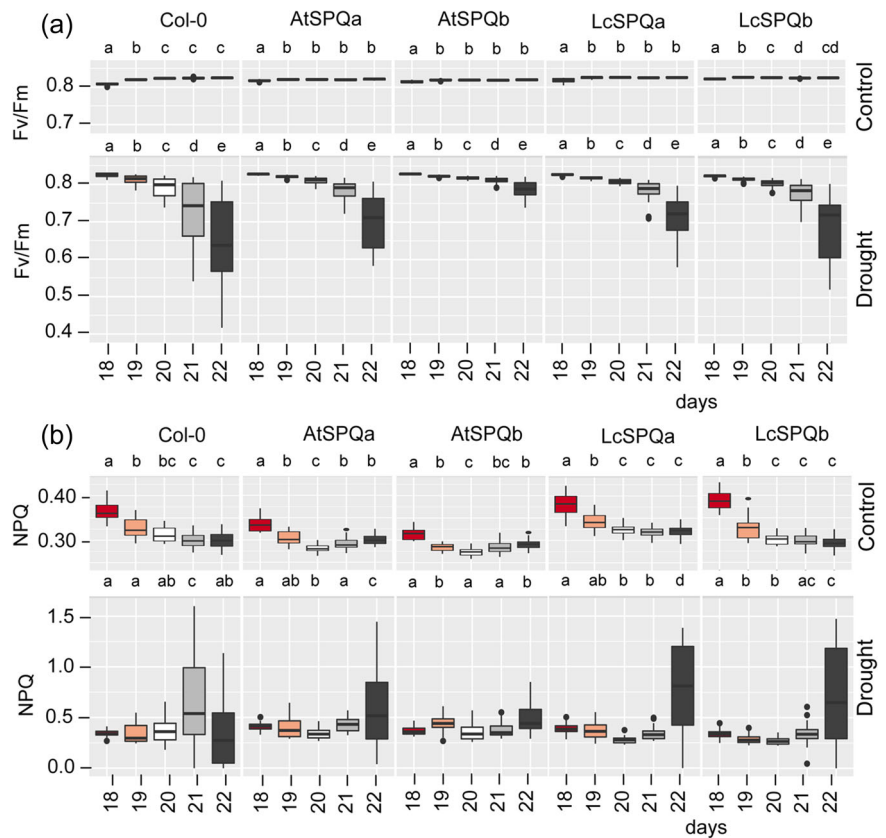
previously published proteins that are implicated in paraquat resistance, suggesting that they are novel players in herbicide resistance. Polyamines were shown to interact with paraquat transport by inhibiting uptake into roots and polyamine transporters were implicated in paraquat absorption in plant cells (Fujita & Shinozaki, 2014; Hart et al., 1992). Mutations in the polyamine transporters *PUT2/PQR2*, the *PUT3/RMV1* or the ABC transporter-coding *PDR11* genes reduced polyamine transport as well as paraquat uptake and toxicity (Dong et al., 2016; Fujita et al., 2012; Xi et al., 2012). Expression of *PUT2*, *PUT3* and *PDR11* genes was, however, not altered in LcSPQ- and AtSPQ-overexpressing plants nor in the *spq1* mutant (Figure S11). Polyamine content in these plants was also similar to wild type and effects of putrescine, spermine and spermidine on root growth were similar in wild-type or transgenic plants (Figure S12). These results suggest that SPQ is not implicated in polyamine metabolism or uptake and paraquat resistance of the overexpressing plants is unrelated to polyamine transport.

ROS generation and oxidative stress are the primary reason for paraquat-induced toxicity and an increase in antioxidant capacity can enhance resistance to this herbicide (Lascano et al., 2012). Mutations that increase tolerance to UV light, salinity, heavy metals or oxidative agents often confer resistance to paraquat also (Hawkes, 2014). Engineering ROS scavenging capacity by overexpression of antioxidant enzymes was shown to improve tolerance to paraquat and reduce oxidative damage in various plants (Kwon et al., 2002; Xu et al., 2013; Yu et al., 2003). The salt-tolerant *pst1* mutant has considerable paraquat resistance and displays enhanced activities of

ROS scavengers such as SOD or APX (Tsugane et al., 1999). The *rcd1* mutant is tolerant to freezing and UVB light and displays enhance resistance to paraquat (Cui et al., 2019; Fujibe et al., 2004). RCD1 is an important component of ROS signalling, which modulates the activity of several ROS-related transcription factors and promotes the activation of the antioxidant system in chloroplasts and therefore alleviates oxidative damage (Ahlfors et al., 2004; Fujibe et al., 2004; Hiltscher et al., 2014). Although SPQ proteins have no similarity to these regulatory genes or ROS scavenging enzymes, paraquat-dependent lipid peroxidation was contained in SPQ-overexpressing plants (Figure 2). H_2O_2 is an important stress and developmental signal, which stimulates the expression of a large set of target genes including *ZAT12*, a master regulator of ROS signalling (Miller et al., 2010). The expression of *RCD1* was not altered in SPQ-overexpressing plants, but paraquat-dependent induction of *ZAT12* was reduced (Figure S11). Further studies are required to define whether limited oxidative damage in SPQ-overexpressing plants is a consequence of reduced ROS generation or enhanced scavenging.

4.2 | SPQ overexpression can enhance drought tolerance

Our results revealed that overexpression of LcSPQ and AtSPQ can enhance, and the *spq1* mutation can reduce ABA sensitivity. Differences in ABA responses have been observed in germination efficiency, plant growth, stomatal closure and expression of several

ABA-induced genes (Figures 5, 6, and S13). It is intriguing how SPQ can interfere with ABA regulation. Crosstalk of paraquat-generated ROS and ABA signalling have already been documented in several plants. Besides being toxic to plant cells, H_2O_2 functions as a potent signalling molecule, modulating a wide range of physiological functions, including responses to abiotic and biotic stresses or plant hormones including ABA (Golldack et al., 2014; Petrov et al., 2012). ABA and paraquat can both induce and regulate the activities of antioxidant enzymes such as SOD, APX and glutathione reductase (GR), and the glutathione–ascorbate antioxidant system, which alleviates paraquat toxicity (Hu et al., 2005; Jiang & Zhang, 2002a; Ozfidan et al., 2012). The rcd1 mutant is resistant to paraquat, but in contrast to SPQ overexpressors, is insensitive to ABA (Ahlfors et al., 2004; Cui et al., 2019; Fujibe et al., 2004). ABA was recently reported to alleviate paraquat-incited cellular damage and help to sustain the photosynthetic activity of paraquat-treated Arabidopsis plants (Cui et al., 2019).

In guard cells, SPQ functioned as a positive regulator of ABA signals. ROS also mediates ABA-induced stomatal closure and is needed for OST1-dependent phosphorylation and activation of SLAC1, an S-type anion channel essential for stomatal closure (Vahisalu et al., 2010). ABA can trigger H_2O_2 accumulation via RBOH/NADPH oxidases needed for activation of Ca^{2+} channels, signal amplification and stomatal closure (Jiang & Zhang, 2002b; Pei et al., 2000; Postiglione & Muday, 2020). Chloroplasts in guard cells were also suggested to generate H_2O_2 in response to ABA signals (Foyer & Harbinson, 1994). ROS generated by photosynthetic electron transport was recently shown to function as signals in ABA-induced stomatal closure (Iwai et al., 2019). ABA generated H_2O_2 signals are also transmitted by MAP kinases MPK3/6 and MPK9, which are implicated in guard cell response to dehydration or pathogen attack (Lee et al., 2016). MAPK signalling can mediate ABA-dependent activation of antioxidant enzymes and reduction of paraquat-generated oxidative damage in maize (Ding et al., 2009). These data indicate that there is intricate crosstalk between ABA and ROS signalling. ABA regulation interferes with paraquat toxicity and oxidative damage and ROS are involved in ABA signalling. SPQ modulates both paraquat and ABA sensitivities, suggesting that it interferes with pathways that connect their action (Figure S21).

Paraquat resistance and ABA hypersensitivity of SPQ-overexpressing plants prompted us to investigate responses to water deprivation, presuming that enhanced response to ABA and alleviated ROS damage may promote tolerance to drought. Diminished oxidative damage, better preserved photosynthetic activity and higher survival rates of LcSPQ- and AtSPQ-overexpressing plants in repeated drought assays confirmed their enhanced viability and tolerance (Figures 7–10 and S14–S20). Faster stomata closure and reduced water evaporation can be direct consequences of ABA hypersensitivity to SPQ overexpression resulting in water-saving in dry environments. RWC was higher in drought-exposed SPQ-overexpressing plants than in wild type (Figure 8). Reduced stomatal conductance in water stress, however, can downregulate photosynthesis, leading to thermal dissipation of energy in the light-harvesting complex and ROS accumulation generating oxidative stress (Chaves et al., 2009; Pinheiro & Chaves, 2011). Overreduction of PSII in photosynthetic electron transport produces superoxide and H_2O_2 during stress, which can also serve as an intracellular messenger in guard cells to promote ABA-induced stomatal closure (Pfannschmidt, 2003; Wang & Song, 2008). Besides modulating stomata aperture, SPQ overexpression could contribute to drought tolerance by reducing oxidative damage. H_2O_2 accumulation and lipid peroxidation were lower in drought-stressed SPQ overexpressing plants than in wild type. As a result, photosynthetic electron transport was less affected (Figures 8 and S19). Despite ABA hypersensitivity, compared to wild type, proline accumulation was reduced in SPQ-overexpressing plants during water stress (Figure 8). Stress-induced proline accumulation is partially controlled by ABA-dependent signals and is also regulated by other factors such as light, energy and redox balance (Alvarez et al., 2022). Inferior proline content of drought-stressed SPQ-overexpressing plants can be the consequence of their higher water content and reduced cellular damage.

Phenotyping various morphological and physiological traits in one experiment can give insights into the dynamics of changes that happen during incremental water stress (Awlia et al., 2016; Rungrat et al., 2016). Plant growth was reduced in SPQ-overexpressing and wild-type plants in a similar manner while rosette roundness showed some differences indicating that drought-related wilting could be reduced in the transgenic plants (Figures 9 and S16). Nondestructive chlorophyll fluorescence imaging can record kinetic changes in photosynthetic activity and give information about the physiological status of the stressed plants even in the absence of visible symptoms (Awlia et al., 2016; Yao et al., 2018). F_v/F_m is a robust parameter that does not change in the early phases of stress, but its sudden decline can indicate differences in viability (Woo et al., 2008). In severe drought conditions, a drop in F_v/F_m values and reduction of ETR in SPQ-overexpressing plants lagged behind wild-type plants indicating their superior photochemical capacity and viability (Figures 10 and S19). In line with these data, SPQ-overexpressing plants survived better severe drought than wild type (Figures 7 and S14). Nonphotochemical parameters such as NPQ reflect the rate of thermal dissipation, an important photoprotective mechanism, which shows dynamic responses to various stresses (Awlia et al., 2016; Yao et al., 2018). NPQ increased more slowly in drought-stressed LcSPQ- and AtSPQ-overexpressing plants than in wild type (Figures 10 and S20). NPQ is an efficient mechanism of photoprotection that is associated with drought responses (Rungrat et al., 2016). A delayed decline in photosynthetic activities of SPQ-overexpressing plants suggests that photosynthesis is better protected in transgenic plants under severe dehydrating conditions.

Better tolerance of SPQ-overexpressing plants to water stress is reflected by improved viability and can be the consequence of enhanced ABA responsiveness, as well as reduced oxidative damage and sustained photosynthetic capacity. SPQs seem to modulate regulatory pathways, which connect ABA and H_2O_2 signals (Figure S21). Interaction of SPQ with proteins implicated in redox

regulation, hormonal and stress signalling suggests that this SP may influence such pathways via protein–protein interactions. A membrane-bound receptor-like protein kinase was identified among the SPQ-interacting proteins, suggesting that it can be implicated in SPQ recognition (Table S1). Precise characterization of such interactions and their functional analysis, however, needs further investigation. Although deciphering the precise biological function of SPQ proteins requires further studies, our data suggest that such SPs can be valuable molecular tools to improve plant performance in arid conditions and help plants to survive periodic droughts.

CONFLICT OF INTEREST

The authors declare no conflict of interest.

DATA AVAILABILITY STATEMENT

The data that support the findings of this study are available in the Supporting Information of this article.

ORCID

Rubén Alcazar https://orcid.org/0000-0002-3567-7586
László Szabados https://orcid.org/0000-0002-9163-9875

REFERENCES

Abraham, E., Hourton-Cabassa, C., Erdei, L. & Szabados, L. (2010) Methods for determination of proline in plants. *Methods in Molecular Biology*, 639, 317–331.

Ahlfors, R., Lang, S., Overmyer, K., Jaspers, P., Brosche, M., Tauriainen, A. et al. (2004) Arabidopsis RADICAL-INDUCED CELL DEATH1 belongs to the WWE protein–protein interaction domain protein family and modulates abscisic acid, ethylene, and methyl jasmonate responses. *The Plant Cell*, 16, 1925–1937.

Alcazar, R., Garcia-Martinez, J.L., Cuevas, J.C., Tiburcio, A.F. & Altabella, T. (2005) Overexpression of ADC2 in Arabidopsis induces dwarfism and late-flowering through GA deficiency. *The Plant Journal*, 43, 425–436.

Alvarez, M.E., Savouré, A. & Szabados, L. (2022) Proline metabolism as regulatory hub. *Trends in Plant Science*, 27, 39–55.

Awlia, M., Nigro, A., Fajkus, J., Schmoeckel, S.M., Negrao, S., Santelia, D. et al. (2016) High-throughput non-destructive phenotyping of traits that contribute to salinity tolerance in *Arabidopsis thaliana*. *Frontiers of Plant Science*, 7, 1414.

Baba, A.I., Rigo, G., Ayaydin, F., Rehman, A.U., Andrasi, N., Zsigmond, L. et al. (2018) Functional analysis of the *Arabidopsis thaliana*
CDPK-related kinase family: AtCRK1 regulates responses to continuous light. *International Journal of Molecular Sciences*, 19, 1282.

Badawi, G.H., Kawano, N., Yamauchi, Y., Shimada, E., Sasaki, R., Kubo, A. et al. (2004) Over-expression of ascorbate peroxidase in tobacco chloroplasts enhances the tolerance to salt stress and water deficit. *Physiologia Plantarum*, 121, 231–238.

Baker, N.R. (2008) Chlorophyll fluorescence: a probe of photosynthesis in vivo. *Annual Review of Plant Biology*, 59, 89–113.

Barr, H.D. & Weatherley, P.E. (1962) A re-examination of the relative turgidity technique for estimating water deficit in leaves. *Australian Journal of Biological Sciences*, 15, 413–428.

Bartels, S. & Boller, T. (2015) Quo vadis, Pep? Plant elicitor peptides at the crossroads of immunity, stress, and development. *Journal of Experimental Botany*, 66, 5183–5193.

Blackburn, M.R., Haruta, M. & Moura, D.S. (2020) Twenty years of progress in physiological and biochemical investigation of RALF peptides. *Plant Physiology*, 182, 1657–1666.

Blanco-Ayala, T., Anderica-Romero, A.C. & Pedraza-Chaverri, J. (2014) New insights into antioxidant strategies against paraquat toxicity. *Free Radical Research*, 48, 623–640.

Bowler, C., Slooten, L., Vandenbranden, S., De Rycke, R., Botterman, J., Sybesma, C. et al. (1991) Manganese superoxide dismutase can reduce cellular damage mediated by oxygen radicals in transgenic plants. *EMBO Journal*, 10, 1723–1732.

Chaves, M.M., Flexas, J. & Pinheiro, C. (2009) Photosynthesis under drought and salt stress: regulation mechanisms from whole plant to cell. *Annali di Botanica*, 103, 551–560.

Chen, J., Yu, F., Liu, Y., Du, C., Li, X., Zhu, S. et al. (2016) FERONIA interacts with ABI2-type phosphatases to facilitate signaling cross-talk between abscisic acid and RALF peptide in Arabidopsis. *Proceedings of the National Academy of Sciences of the United States of America*, 113, E5519–E5527.

Chiang, H.C., Lo, J.C. & Yeh, K.C. (2006) Genes associated with heavy metal tolerance and accumulation in Zn/Cd hyperaccumulator *Arabidopsis halleri*: a genomic survey with cDNA microarray. *Environmental Science and Technology*, 40, 6792–6798.

Clough, S.J. & Bent, A.F. (1998) Floral dip: a simplified method for Agrobacterium-mediated transformation of *Arabidopsis thaliana*. *The Plant Journal*, 16, 735–743.

Cocheme, H.M. & Murphy, M.P. (2008) Complex I is the major site of mitochondrial superoxide production by paraquat. *Journal of Biological Chemistry*, 283, 1786–1798.

Cui, F., Brosche, M., Shapiguzov, A., He, X.Q., Vainonen, J.P., Leppala, J. et al. (2019) Interaction of methyl viologen-induced chloroplast and mitochondrial signalling in Arabidopsis. *Free Radical Biology and Medicine*, 134, 555–566.

Cummins, I., Cole, D.J. & Edwards, R. (1999) A role for glutathione transferases functioning as glutathione peroxidases in resistance to multiple herbicides in black-grass. *The Plant Journal*, 18, 285–292.

Ding, H.D., Zhang, X.H., Xu, S.C., Sun, L.L., Jiang, M.Y., Zhang, A.Y. et al. (2009) Induction of protection against paraquat-induced oxidative damage by abscisic acid in maize leaves is mediated through mitogen-activated protein kinase. *Journal of Integrative Plant Biology*, 51, 961–972.

Dong, S., Hu, H., Wang, Y., Xu, Z., Zha, Y., Cai, X. et al. (2016) A pqr2 mutant encodes a defective polyamine transporter and is negatively affected by ABA for paraquat resistance in *Arabidopsis thaliana*. *Journal of Plant Research*, 129, 899–907.

Faragó, D., Sass, L., Valkai, I., Andrási, N. & Szabados, L. (2018) PlantSize offers an affordable, non-destructive method to measure plant size and color in vitro. *Frontiers of Plant Science*, 9, 219.

Ferrando, A., Farras, R., Jasik, J., Schell, J. & Koncz, C. (2000) Intron-tagged epitope: a tool for facile detection and purification of proteins expressed in Agrobacterium-transformed plant cells. *The Plant Journal*, 22, 553–560.

Finkelstein, R. (2013) Abscisic acid synthesis and response. *The Arabidopsis Book*, 11, e0166.

Fiume, E., Guyon, V., Remoué, C., Magnani, E., Miquel, M., Grain, D. et al. (2016) TWS1, a novel small protein, regulates various aspects of seed and plant development. *Plant Physiology*, 172, 1732–1745.

Foyer, C.H. & Harbinson, J. (1994) Oxygen metabolism and the regulation of photosynthetic electron transport. In: Foyer, C.H. & Mullineaux, P. M. (Eds.) *Causes of photooxidatives stress and amelioration of defense systems in plants*. Boca Raton: CRC Press, pp. 1–42.

Fujibe, T., Saji, H., Arakawa, K., Yabe, N., Takeuchi, Y. & Yamamoto, K.T. (2004) A methyl viologen-resistant mutant of Arabidopsis, which is allelic to ozone-sensitive rcd1, is tolerant to supplemental ultraviolet-B irradiation. *Plant Physiology*, 134, 275–285.

Fujita, M., Fujita, Y., Iuchi, S., Yamada, K., Kobayashi, Y., Urano, K. et al. (2012) Natural variation in a polyamine transporter determines paraquat tolerance in Arabidopsis. *Proceedings of the National Academy of Sciences of the United States of America*, 109, 6343–6347.

Fujita, M. & Shinozaki, K. (2014) Identification of polyamine transporters in plants: paraquat transport provides crucial clues. *Plant and Cell Physiology*, 55, 855–861.

Golldack, D., Li, C., Mohan, H. & Probst, N. (2014) Tolerance to drought and salt stress in plants: unraveling the signaling networks. *Frontiers of Plant Science*, 5, 151.

Gressel, J. (1984) Evolution of herbicide-resistant weeds. *CIBA Foundation Symposium*, 102, 73–93.

Hart, J.J., Ditomaso, J.M., Linscott, D.L. & Kochian, L.V. (1992) Transport interactions between paraquat and polyamines in roots of intact maize seedlings. *Plant Physiology*, 99, 1400–1405.

Hawkes, T.R. (2014) Mechanisms of resistance to paraquat in plants. *Pest Management Science*, 70, 1316–1323.

Hiltscher, H., Rudnik, R., Shaikhali, J., Heiber, I., Mellenthin, M., Meirelles Duarte, I. et al. (2014) The radical induced cell death protein 1 (RCD1) supports transcriptional activation of genes for chloroplast antioxidant enzymes. *Frontiers of Plant Science*, 5, 475.

Hu, X., Jiang, M., Zhang, A. & Lu, J. (2005) Abscisic acid-induced apoplastic H2O2 accumulation up-regulates the activities of chloroplastic and cytosolic antioxidant enzymes in maize leaves. *Planta*, 223, 57–68.

Hubner, N.C., Bird, A.W., Cox, J., Splettstoesser, B., Bandilla, P., Poser, I. et al. (2010) Quantitative proteomics combined with BAC TransgeneOmics reveals in vivo protein interactions. *Journal of Cell Biology*, 189, 739–754.

Iwai, S., Ogata, S., Yamada, N., Onjo, M., Sonoike, K. & Shimazaki, K.I. (2019) Guard cell photosynthesis is crucial in abscisic acid-induced stomatal closure. *Plant Direct*, 3, e00137.

Jankovics, F., Bence, M., Sinka, R., Farago, A., Bodai, L., Pettko-Szandtner, A. et al. (2018) Drosophila small ovary gene is required for transposon silencing and heterochromatin organization, and ensures germline stem cell maintenance and differentiation. *Development*, 145. dev170639

Jiang, M. & Zhang, J. (2002a) Involvement of plasma-membrane NADPH oxidase in abscisic acid- and water stress-induced antioxidant defense in leaves of maize seedlings. *Planta*, 215, 1022–1030.

Jiang, M. & Zhang, J. (2002b) Water stress-induced abscisic acid accumulation triggers the increased generation of reactive oxygen species and up-regulates the activities of antioxidant enzymes in maize leaves. *Journal of Experimental Botany*, 53, 2401–2410.

Jóri, B., SoÓs, V., Szegő, D., Páldi, E., Szigeti, Z., Rácz, I. et al. (2007) Role of transporters in paraquat resistance of horseweed Conyza canadensis (L.) Cronq. *Pesticide Biochemistry and Physiology*, 88, 57–65.

Julkowska, M.M., Saade, S., Agarwal, G., Gao, G., Pailles, Y., Morton, M. et al. (2019) MVApp—multivariate analysis application for streamlined data analysis and curation. *Plant Physiology*, 180, 1261–1276.

Kasukabe, Y., He, L., Nada, K., Misawa, S., Ihara, I. & Tachibana, S. (2004) Overexpression of spermidine synthase enhances tolerance to multiple environmental stresses and up-regulates the expression of various stress-regulated genes in transgenic Arabidopsis thaliana. *Plant and Cell Physiology*, 45, 712–722.

Kereszt, A., Mergaert, P., Montiel, J., Endre, G. & Kondorosi, É. (2018) Impact of plant peptides on symbiotic nodule development and functioning. *Frontiers in Plant Science*, 9, 1026.

Kim, J.S., Jeon, B.W. & Kim, J. (2021) Signaling peptides regulating abiotic stress responses in plants. *Frontiers in Plant Science*, 12, 704490.

Kobayashi, K., Suzuki, T., Iwata, E., Nakamichi, N., Suzuki, T., Chen, P. et al. (2015) Transcriptional repression by MYB3R proteins regulates plant organ growth. *EMBO Journal*, 34, 1992–2007.

Koncz, C., Martini, N., Szabados, L., Hrouda, M., Bachmair, A. & Schell, J. (1994) Specialized vectors for gene tagging and expression studies. In: Gelvin, S.B. (Ed.) *Plant molecular biology manual*, volume B1. Dordrecht: Kluwer Academic Publishers, pp. 53–74.

Krall, J., Bagley, A.C., Mullenbach, G.T., Hallewell, R.A. & Lynch, R.E. (1988) Superoxide mediates the toxicity of paraquat for cultured mammalian cells. *Journal of Biological Chemistry*, 263, 1910–1914.

Kurepa, J., Smalle, J., Van Montagu, M. & Inze, D. (1998) Polyamines and paraquat toxicity in Arabidopsis thaliana. *Plant and Cell Physiology*, 39, 987–992.

Kwon, S.-J., Jeong, Y.J., Lee, H.-S., Kim, J.S., Cho, K.-Y., Allen, R.D. et al. (2002) Enhanced tolerances of transgenic tobacco plants expressing both superoxide dismutase and ascorbate peroxidase in chloroplasts against methyl viologen-mediated oxidative stress. *Plant, Cell and Environment*, 25, 873–882.

Lång, V. & Palva, E.T. (1992) The expression of a rab-related gene, rab18, is induced by abscisic acid during the cold acclimation process of Arabidopsis thaliana (L.) Heynh. *Plant Molecular Biology*, 20, 951–962.

Lasat, M.M., DiTomaso, J.M., Hart, J.J. & Kochian, L.V. (1997) Evidence for vacuolar sequestration of paraquat in roots of a paraquat-resistant Hordeum glaucum biotype. *Physiologia Plantarum*, 99, 255–262.

Lascano, R., Munoz, N., Robert, G., Rodriguez, M., Melchiore, M., Trippi, V. et al. (2012) Paraquat: an oxidative stress inducer. *Herbicides—Properties, Synthesis and Control of Weeds*, 135–148.

Lee, Y., Kim, Y.J., Kim, M.H. & Kwak, J.M. (2016) MAPK Cascades in guard cell signal transduction. *Frontiers in Plant Science*, 7, 80.

Lee, Y.P., Kim, S.H., Bang, J.W., Lee, H.S., Kwak, S.S. & Kwon, S.Y. (2007) Enhanced tolerance to oxidative stress in transgenic tobacco plants expressing three antioxidant enzymes in chloroplasts. *Plant Cell Reports*, 26, 591–598.

Li, J., Mu, J., Bai, J., Fu, F., Zou, T., An, F. et al. (2013) Paraquat Resistant1, a Golgi-localized putative transporter protein, is involved in intracellular transport of paraquat. *Plant Physiology*, 162, 470–483.

Livak, K.J. & Schmittgen, T.D. (2001) Analysis of relative gene expression data using real-time quantitative PCR and the 2(−Delta Delta C(T)) Method. *Methods*, 25, 402–408.

Marcé, M., Brown, D.S., Capell, T., Figueras, X. & Tiburcio, A.F. (1995) Rapid high-performance liquid chromatographic method for the quantitation of polyamines as their dansyl derivatives: application to plant and animal tissues. *Journal of Chromatography*, 666, 329–335.

Marco, F., Alcazar, R., Tiburcio, A.F. & Carrasco, P. (2011) Interactions between polyamines and abiotic stress pathway responses unraveled by transcriptome analysis of polyamine overproducers. *OMICS*, 15, 775–781.

Miller, G., Suzuki, N., Ciftci-Yilmaz, S. & Mittler, R. (2010) Reactive oxygen species homeostasis and signalling during drought and salinity stresses. *Plant, Cell and Environment*, 33, 453–467.

Msanne, J., Lin, J., Stone, J.M. & Awada, T. (2011) Characterization of abiotic stress-responsive Arabidopsis thaliana RD29A and RD29B genes and evaluation of transgenes. *Planta*, 234, 97–107.

Murgia, I., Tarantino, D., Vannini, C., Bracale, M., Carravieri, S. & Soave, C. (2004) Arabidopsis thaliana plants overexpressing thylakoidal ascorbate peroxidase show increased resistance to Paraquat-induced photooxidative stress and to nitric oxide-induced cell death. *The Plant Journal*, 38, 940–953.

Mustilli, A.C., Merlot, S., Vavasseur, A., Fenzi, F. & Giraudat, J. (2002) Arabidopsis OST1 protein kinase mediates the regulation of

stomatal aperture by abscisic acid and acts upstream of reactive oxygen species production. *The Plant Cell*, 14, 3089–3099.

Norman, M.A., Fuerst, E.P., Smeda, R.J. & Vaughn, K.C. (1993) Evaluation of paraquat resistance mechanisms in conyza. *Pesticide Biochemistry and Physiology*, 46, 236–249.

Ozfidan, C., Turkan, I., Sekmen, A.H. & Seckin, B. (2012) Abscisic acid-regulated responses of aba2-1 under osmotic stress: the abscisic acid-inducible antioxidant defence system and reactive oxygen species production. *Plant Biology (Stuttg)*, 14, 337–346.

Patharkar, O.R. & Walker, J.C. (2016) Core mechanisms regulating developmentally timed and environmentally triggered abscission. *Plant Physiology*, 172, 510–520.

Pavicic, M., Mouhu, K., Wang, F., Bilicka, M., Chovanček, E. & Himanen, K. (2017) Genomic and phenomic screens for flower related RING type ubiquitin E3 ligases in Arabidopsis. *Frontiers in Plant Science*, 8, 416.

Pei, Z.M., Murata, Y., Benning, G., Thomine, S., Klusener, B., Allen, G.J. et al. (2000) Calcium channels activated by hydrogen peroxide mediate abscisic acid signalling in guard cells. *Nature*, 406, 731–734.

Petrov, V.D. & Van Breusegem, F. (2012) Hydrogen peroxide-a central hub for information flow in plant cells. *AoB Plants*, 2012. 2012 pls014.

Pfannschmidt, T. (2003) Chloroplast redox signals: how photosynthesis controls its own genes. *Trends in Plant Science*, 8, 33–41.

Pinheiro, C. & Chaves, M.M. (2011) Photosynthesis and drought: can we make metabolic connections from available data? *Journal of Experimental Botany*, 62, 869–882.

Postiglione, A.E. & Muday, G.K. (2020) The role of ROS homeostasis in ABA-induced guard cell signaling. *Frontiers in Plant Science*, 11, 968.

Preston, C., Holtum, J.A. & Powles, S.B. (1991) Resistance to the herbicide paraquat and increased tolerance to photoinhibition are not correlated in several weed species. *Plant Physiology*, 96, 314–318.

Rigo, G., Valkai, I., Farago, D., Kiss, E., Van Houdt, S., Van de Steene, N. et al. (2016) Gene mining in halophytes: functional identification of stress tolerance genes in *Lepidium crassifolium*. *Plant, Cell and Environment*, 39, 2074–2084.

Rungrat, T., Awlia, M., Brown, T., Cheng, R., Sirault, X., Fajkus, J. et al. (2016) Using phenomic analysis of photosynthetic function for abiotic stress response gene discovery. *The Arabidopsis Book*, 14, e0185.

Shaaltier, Y., Glazer, A., Bocion, P.F. & Gressel, J. (1988) Cross tolerance to herbicidal and environmental oxidants of plant biotypes tolerant to paraquat, sulfur dioxide, and ozone. *Pesticide Biochemistry and Physiology*, 31, 13–23.

Sperdouli, I. & Moustakas, M. (2011) Spatio-temporal heterogeneity in *Arabidopsis thaliana* leaves under drought stress. *Plant Biology (Stuttg)*, 14, 118–128.

Szabados, L. & Koncz, C. (2003) Identification of T-DNA insertions in Arabidopsis genes. In: Prade, R.A. & Bohnert, H.J. (Eds.) *Genomics of plants and fungi*. New York: Marcel Dekker Inc, pp. 255–277.

Szabados, L., Kovacs, I., Oberschall, A., Abraham, E., Kerekes, I., Zsigmond, L. et al. (2002) Distribution of 1000 sequenced T-DNA tags in the Arabidopsis genome. *The Plant Journal*, 32, 233–242.

Szabados, L. & Savoure, A. (2010) Proline: a multifunctional amino acid. *Trends in Plant Science*, 15, 89–97.

Szigeti, Z., Racz, I. & Lasztity, D. (2001) Paraquat resistance of weeds--the case of *Conyza canadensis* (L.) Cronq. *Zeitschrift fur Naturforschung C*, 56, 319–328.

Takahashi, F., Hanada, K., Kondo, T. & Shinozaki, K. (2019) Hormone-like peptides and small coding genes in plant stress signaling and development. *Current Opinion in Plant Biology*, 51, 88–95.

Takahashi, F., Suzuki, T., Osakabe, Y., Betsuyaku, S., Kondo, Y., Dohmae, N. et al. (2018) A small peptide modulates stomatal control via abscisic acid in long-distance signalling. *Nature*, 556, 235–238.

Tsugane, K., Kobayashi, K., Niwa, Y., Ohba, Y., Wada, K. & Kobayashi, H. (1999) A recessive Arabidopsis mutant that grows photoautotrophically under salt stress shows enhanced active oxygen detoxification. *The Plant Cell*, 11, 1195–1206.

Vahisalu, T., Puzõrjova, I., Brosché, M., Valk, E., Lepiku, M., Moldau, H. et al. (2010) Ozone-triggered rapid stomatal response involves the production of reactive oxygen species, and is controlled by SLAC1 and OST1. *The Plant Journal*, 62, 442–453.

Vie, A.K., Najafi, J., Winge, P., Cattan, E., Wrzaczek, M., Kangasjarvi, J. et al. (2017) The IDA-LIKE peptides IDL6 and IDL7 are negative modulators of stress responses in *Arabidopsis thaliana*. *Journal of Experimental Botany*, 68, 3557–3571.

Wang, P. & Song, C.P. (2008) Guard-cell signalling for hydrogen peroxide and abscisic acid. *New Phytologist*, 178, 703–718.

Woo, N.S., Badger, M.R. & Pogson, B.J. (2008) A rapid, non-invasive procedure for quantitative assessment of drought survival using chlorophyll fluorescence. *Plant Methods*, 4, 27.

Xi, J., Xu, P. & Xiang, C.B. (2012) Loss of AtPDR11, a plasma membrane-localized ABC transporter, confers paraquat tolerance in *Arabidopsis thaliana*. *The Plant Journal*, 69, 782–791.

Xu, J., Duan, X., Yang, J., Beeching, J.R. & Zhang, P. (2013) Enhanced reactive oxygen species scavenging by overproduction of superoxide dismutase and catalase delays postharvest physiological deterioration of cassava storage roots. *Plant Physiology*, 161, 1517–1528.

Yamaguchi, Y. & Huffaker, A. (2011) Endogenous peptide elicitors in higher plants. *Current Opinion in Plant Biology*, 14, 351–357.

Yao, J., Sun, D., Cen, H., Xu, H., Weng, H., Yuan, F. et al. (2018) Phenotyping of Arabidopsis drought stress response using kinetic chlorophyll fluorescence and multicolor fluorescence imaging. *Frontiers in Plant Science*, 9, 603.

Yoshimura, K., Miyao, K., Gaber, A., Takeda, T., Kanaboshi, H., Miyasaka, H. et al. (2004) Enhancement of stress tolerance in transgenic tobacco plants overexpressing Chlamydomonas glutathione peroxidase in chloroplasts or cytosol. *The Plant Journal*, 37, 21–33.

Yu, Q., Cairns, A. & Powles, S. (2007) Glyphosate, paraquat and ACCase multiple herbicide resistance evolved in a *Lolium rigidum* biotype. *Planta*, 225, 499–513.

Yu, T., Li, Y.S., Chen, X.F., Hu, J., Chang, X. & Zhu, Y.G. (2003) Transgenic tobacco plants overexpressing cotton glutathione S-transferase (GST) show enhanced resistance to methyl viologen. *Journal of Plant Physiology*, 160, 1305–1311.

Yu, X., Huang, S. & Powles, S. (2010) Direct measurement of paraquat in leaf protoplasts indicates vacuolar paraquat sequestration as a resistance mechanism in *Lolium rigidum*. *Pesticide Biochemistry and Physiology*, 98, 104–109.

Zhang, L., Shi, X., Zhang, Y., Wang, J., Yang, J., Ishida, T. et al. (2019) CLE9 peptide-induced stomatal closure is mediated by abscisic acid, hydrogen peroxide, and nitric oxide in *Arabidopsis thaliana*. *Plant, Cell and Environment*, 42, 1033–1044.

Zhou, J., Wang, J., Li, X., Xia, X.J., Zhou, Y.H., Shi, K. et al. (2014) H_2O_2 mediates the crosstalk of brassinosteroid and abscisic acid in tomato responses to heat and oxidative stresses. *Journal of Experimental Botany*, 65, 4371–4383.

SUPPORTING INFORMATION

Additional supporting information can be found online in the Supporting Information section at the end of this article.